

VITOR ALENCAR NUNES

Compatibility and adhesion between fiber-reinforced alkali-activated repair mortar and concrete substrate

Dissertação de Mestrado

Departamento de Engenharia Civil

Belo Horizonte, janeiro de 2018

VITOR ALENCAR NUNES

**COMPATIBILITY AND ADHESION BETWEEN FIBER-
REINFORCED ALKALI-ACTIVATED REPAIR MORTAR AND
CONCRETE SUBSTRATE**

Dissertation presented to the Postgraduate Programme in Civil Engineering at the Federal Center for Technological Education of Minas Gerais, as partial requirement to obtain the Master of Science (M.Sc.) degree in Civil Engineering.

Supervisor: Prof. Dr. Paulo Henrique Ribeiro Borges

Co-supervisor: Prof. Dr. Cristina Zanotti

Belo Horizonte, 15 de janeiro de 2018

Nunes, Vitor Alencar
N972c Compatibility and adhesion between fiber-reinforced alkali-activated repair mortar and concrete substrate / Vitor Alencar Nunes. – 2018.
62 f. : il., gráfs, tabs., fotos.

Dissertação apresentada ao Programa de Pós-Graduação em Engenharia de Civil.
Orientador: Paulo Henrique Ribeiro Borges.
Coorientadora: Cristina Zanotti.
Bibliografia: f. 57-62.
Dissertação (mestrado) – Centro Federal de Educação Tecnológica de Minas Gerais, Departamento de Engenharia Civil

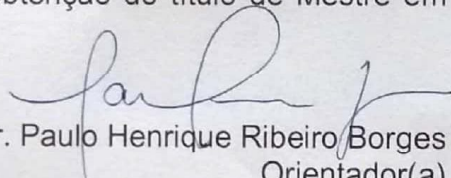
1. Reações agregadas alcalinas – Teses. 2. Argamassa – Manutenção e reparos – Teses. 3. Aderência – Teses. 4. Compostos fibrosos – Teses. I. Borges, Paulo Henrique Ribeiro. II. Zanotti, Cristina. III. Centro Federal de Educação Tecnológica de Minas Gerais. Departamento de Engenharia Civil. IV. Título.

CDD 691.3

VITOR ALENCAR NUNES

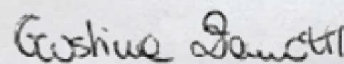
**COMPATIBILITY AND ADHESION BETWEEN FIBER-
REINFORCED ALKALI-ACTIVATED REPAIR MORTAR AND
CONCRETE SUBSTRATE**

Dissertação apresentada ao Programa de Pós-
Graduação em Engenharia Civil do CEFET-MG como
requisito parcial para obtenção do título de Mestre em
Engenharia Civil



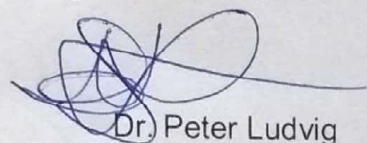
Dr. Paulo Henrique Ribeiro Borges
Orientador(a)

Departamento de Engenharia Civil, CEFET-MG



Dr. Cristina Zanotti
Coorientador(a)

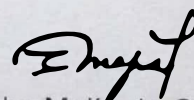
Departamento de Engenharia Civil, UBC



Dr. Peter Ludvig

Departamento de Engenharia Civil, CEFET-MG

|



Dr. Ruby Mejía de Gutiérrez
Departamento de Engenharia de Materiais, Universidade del Valle

Belo Horizonte, 15 de Janeiro de 2018

"Innovation distinguishes between a leader and a follower"

Steve Jobs

ACKLOGDMENTS

First of all, I thank God for always enlightening my path, helping me make the best choices, in addition to the strength and determination during difficult times along this walk.

I thank my family, Angelo, Cristiana and Luiz, my great friends and examples of life, for all the support and encouragement along the way. Thanks for all the knowledge shared and incentive seeking the perfection.

I thank to CEFET-MG and to CAPES to provide and finance the research. In special to all members of our research group in alternative materials and the laboratory work team, due to the assistance during the development of this work.

And finally, I thank my two supervisors, Professor Paulo Borges and Professor Cristina Zanotti, for all the help, teaching, fellowship and friendship throughout the development of this research.

ABSTRACT

Concrete repairing is a complex task that requires a special knowledge of technical building regulations and standards, deterioration mechanism and diagnosis, repair principles and methods, repair materials, execution of repair works, inspections, monitoring and maintenance. So far, most used patch repair mortars fall into two categories, (i) the mortars based on inorganic binders (Portland cement, PC) and (ii) those based on organic binders (polymers). Recent investigations reveal a third category of mortars with high potential to be used in the field of concrete repair, i.e. the alkali-activated based mortars. Alkali-activated materials (AAM) have been widely promoted as a greener binder for sustainable constructions. These binders can be generated from a wide range of aluminosilicate materials under alkaline conditions to produce a hardened component. This study, therefore, aims to evaluate the compatibility and the adhesion between a fiber-reinforced alkali-activated mortar and a concrete substrate. Different formulations of AAM were initially studied, based on the alkaline activation of metakaolin (MK) and blast furnace slag (BFS); their mechanical properties and modulus of elasticity were assessed. Five formulations were selected after this preliminary evaluation in order to produce the repair mortar and to apply onto concrete substrates. A volume fraction of 0.25% of PP fiber was used to mitigate the early-age shrinkage and to increase the adhesion bond of the repair mortar with the concrete substrate. The bond strength was evaluated by pull-off testing. The crack and delamination behaviour were assessed by four-point bending tests. Physical properties were also investigated: water absorption, apparent porosity and apparent density. Results showed a good compatibility and adhesion between alkali-activated repair mortars and the PC substrate. Satisfactory bond strengths were found meeting the required by the structure repair standard BS EN 1504. The delamination issue was observed only in 100 % MK-based mortars and the crack propagation behaviour was typical from brittle materials. The formulation 80MK-20BFS designed with $\text{SiO}_2/\text{Al}_2\text{O}_3$ molar ratio 3.0 and fiber-reinforced was selected as the most promising one to structural repair proposes.

Key-words: Alkali-activated materials, repair mortar, structural repair, adhesion, fiber-reinforced composite.

RESUMO

O reparo de estruturas de concreto é uma tarefa complexa que requer um conhecimento especial de regulamentos e normas técnica de construção, mecanismo de deterioração, princípios e métodos de reparo, materiais de reparo, execução de trabalhos de reparo, inspeções, monitoramento e manutenção. Até o momento, as argamassas de reparo mais utilizadas se dividem em duas categorias, (i) as argamassas baseadas em ligantes inorgânicos (cimento Portland) e (ii) as baseadas em ligantes orgânicos (polímeros). Pesquisas recentes revelam uma terceira categoria de argamassas com alto potencial para serem utilizadas como reparo de concreto; as argamassas álcali-ativadas. Os materiais álcali-ativados (MAA) vêm sendo amplamente promovidos como um ligante mais verde para construções sustentáveis. Estes ligantes podem ser obtidos a partir da ativação alcalina de uma ampla variedade de aluminossilicatos para a produção de componentes endurecidos. Este estudo, portanto, visa avaliar a compatibilidade e a aderência entre argamassas álcali-ativadas reforçadas com fibra e um substrato de concreto. Diferentes formulações de MAA foram inicialmente estudadas, com base na ativação alcalina de metacaulim (MK) e de escória do alto-forno (BFS); suas propriedades mecânicas e seu módulo de elasticidade foram avaliados. Cinco formulações foram selecionadas para a produção de argamassas de reparo e aplicação sobre substratos de concreto. Uma fração 0,25% de fibra de PP foi utilizada para mitigar a retração em pequenas idades e aumentar aderência da argamassa. A aderência foi medida pelo ensaio de *pull-off*. Os comportamentos de fissuração e delaminação foram avaliados pelo mecanismo “*crack trapping*”. As propriedades físicas também foram estudadas: absorção de água, porosidade aparente e densidade aparente. Os resultados apresentaram uma boa compatibilidade e aderência entre as argamassas de reparo e o substrato. Resistências à aderência satisfatórias foram encontradas, atendendo os requisitos da norma de reparo BS EN 1504. O problema de delaminação foi observado apenas na argamassa com 100% de MK e o comportamento de fissuração foi típico de materiais frágeis. A formulação 80MK-20BFS com razão molar $\text{SiO}_2/\text{Al}_2\text{O}_3$ de 3.0 e reforçada com fibra foi selecionada como a mais promissora para o uso em reparo de estruturas de concreto.

Palavras-chave: materiais álcali-ativados, argamassa de reparo, reparo estrutural, aderência, compósitos reforçados com fibra.

LIST OF FIGURES

Figure 1 – Classification of AAM's and comparisons concerning chemistry (PROVIS & VAN DEVENTER, 2014)	4
Figure 2 – Process and reaction products of different type activation (PROVIS & BERNAL, 2014B).....	5
Figure 3 – View of the three-dimensional structure of a N-A-S-H gel (GARCIA-LODEIRO <i>et al.</i> , 2015)	7
Figure 4 – Types of gel structures (DAVIDOVITS, 1994)	7
Figure 5 – Pathways for the conversion of kaolinite (PROVIS & BERNAL, 2014B).....	8
Figure 6 – Logical sequence (phases) of repair projects (RAUPACH & BUTTNER, 2014)	11
Figure 7 – Common causes of damages in structures (RAUPACH & BUTTNER, 2014)	11
Figure 8 – Factors that influence the durability of repair materials (EMMONS <i>et al.</i> , 1993)	15
Figure 9 – Scheme with the dolly distribution (EN, 1999)	18
Figure 10 – Dimension of specimen and loading configuration for a crack trapping mechanism test (LIM & LI, 1997).....	19
Figure 11 – Load-displacement curve (LIM & LI, 1997).....	20
Figure 12 – Flowchart of the experimental program.....	23
Figure 13 – Shimadzu XRD-7000 equipment.....	24
Figure 14 – CILAS 1090 LASER particle size analyser.....	25
Figure 15 – Pycnometry equipment.....	25
Figure 16 – Curing process of the concrete substrates before demolding	26
Figure 17 – Water blasting process.....	27
Figure 18 – Prepared surface of the concrete substrates.....	27
Figure 19 – Water tank for curing process of the concrete substrates	27
Figure 20 – (a) Circular saw; (b) and (c) samples after surface preparation	28
Figure 21 – Final preparation of the beams substrates	28
Figure 22 – Flow table test	30
Figure 23 – (a) Metkon saw; (b) samples before and (c) after surface preparation ..	31
Figure 24 – Alkali-activated mortar: (a) and (b) being applied and (c) after vibrating process.....	32
Figure 25 - Mixing process of the repair mortar beams	33

Figure 26 - (a) Substrate in metallic form; (b) casting of the AAM and (c) compaction process.....	33
Figure 27 – Universal press used for mechanical tests	34
Figure 28 – Loading schematic representation to determinate the modulus of elasticity (adapted from (ABNT, 2008))	34
Figure 29 – Modulus of elasticity test for (a) concrete and (b) alkali-activated mortars	35
Figure 30 – Drilling process.....	36
Figure 31 – Setting the dollies distribution on the substrate-repair panel.....	36
Figure 32 – Pull-off test	37
Figure 33 – Four point bending test.....	37
Figure 34 – Diffractometer: (a) MK and (b) BFS.....	39
Figure 35 – Particle size distribution of MK and BFS	40
Figure 36 – Dolomite aggregate particle size distribution.....	41
Figure 37 – Compressive strength versus $[\text{SiO}_2] / [\text{Al}_2\text{O}_3]$ molar ratio for alkali-activated mortars.....	42
Figure 38 – Modulus of elasticity versus $[\text{SiO}_2] / [\text{Al}_2\text{O}_3]$ molar ratio.....	43
Figure 39 – Bond strength results obtained by pull-off test	46
Figure 40 - Failure samples after pull-off test: (I) A : A/B, (II) A : A/B : B, (III) B and (IV) A/B.....	47
Figure 41 – Load x displacement curves.....	48
Figure 42 – (a) flexural tensile test and (b) detail of a fiber-reinforced cracking beam	48
Figure 43 – Flexural strength of both beams of each formulation	49
Figure 44 – Cracking pattern after bending test (for each formulation: left side - no fiber; right side - fiber reinforced).....	50
Figure 45 – Delamination problem: (a) fissured interface before test and (b) failure beam with high delamination on the interface	50
Figure 46 – Water absorption and apparent porosity	52
Figure 47 – Apparent density and solution/binder ratio versus % of BFS.....	53

LIST OF TABLES

Table 1 – Structural compatibility between substrate and repair mortars	16
Table 2 – Standard adhesion bond requirement	18
Table 3 – Studied formulations.....	29
Table 4 – Raw materials chemical composition	39
Table 5 – Consistency of fresh mortars.....	41
Table 6 – Chosen formulations properties.....	44
Table 7 – Bond strength results	45

SUMMARY

1.	INTRODUCTION.....	1
1.1.	OBJECTIVES.....	2
2.	LITERATURE REVIEW	3
2.1.	ALKALI-ACTIVATED MATERIALS	3
2.1.1.	High calcium alkali-activated materials.....	5
2.1.2.	Low-calcium and calcium-free alkali-activated materials.....	6
2.1.3.	Blended alkali-activated systems	8
2.2.	CONCRETE STRUCTURAL REPAIR.....	10
2.2.1.	European Standard - EN 1504.....	10
2.2.2.	Conventional materials as repair mortars.....	12
2.2.3.	Alkali-activated materials as potential repair materials	13
2.3.	SUBSTRATE-REPAIR COMPATIBILITY	15
2.4.	SUBSTRATE-REPAIR ADHESION	17
2.4.1.	Bond strength by pull-off test - British Standard (BS EN 1542).....	17
2.4.2.	Crack Trapping Mechanism Test	19
2.5.	USE OF FIBERS IN STRUCTURAL REPAIR	20
3.	METHODOLOGY.....	22
3.1.	SCOPE OF THIS STUDY	22
3.2.	MATERIAL AND METHODS.....	24
3.2.1.	Materials.....	24
3.2.2.	Concrete substrates preparation	26
3.2.2.1.	Substrate for the pull-off test.....	26
3.2.2.2.	Substrate for the four-point bending test.....	28
3.2.3.	Alkali-activated repair formulations	29
3.2.4.	Alkali-activated mortars preparation	30

3.2.5.	Substrate-repair panels preparation.....	31
3.2.6.	Substrate-repair beams preparation.....	32
3.2.7.	Mechanical evaluation	33
3.2.8.	Substrate-repair adhesion evaluation	35
3.2.8.1.	Bond strength by pull-off test	35
3.2.8.2.	Crack Trapping Mechanism by four point bending.....	37
3.2.9.	Physical evaluation	38
4.	RESULTS	39
4.1.	CHARACTERIZATION OF RAW MATERIALS	39
4.2.	COMPATIBILITY	41
4.2.1.	Fresh Properties.....	41
4.2.2.	Mechanical Properties	42
4.3.	ADHESION PROPERTIES	44
4.3.1.	Pull-Off test.....	44
4.3.2.	Crack Trapping Mechanism Test	47
4.4.	PHYSICAL PROPERTIES	51
5.	CONCLUNDING REMARKS	54

1. INTRODUCTION

In the recent years the amount of concrete repair has significantly increased since many existing concrete buildings and structures have been deteriorated due to exposure to severe climate and work conditions for long periods of time (RAUPACH & BUTTNER, 2014; KRAMAR *et al.*, 2016). Many of those degraded concrete structures were built decades ago when little attention was given to durability issues, which resulted in aesthetic, functional or structural problems (PACHECO-TORGAL *et al.*, 2012).

Thereby, the infrastructure rehabilitation represents a great opportunity of development for the construction industry. However, the diagnosis, design, selection of products and execution of repair works need to be adjusted to each individual structure conditions, requiring special knowledge (RAUPACH & BUTTNER, 2014). The patch repair method is widely used to restore the original conditions of the concrete structure; the most used repair materials are based on Portland cement (PC) or polymers (PACHECO-TORGAL *et al.*, 2012).

Alkali-activated materials (AAM) have been considered as potential repair materials. They are synthesized by the condensation of aluminosilicates structures. Highly alkaline solutions like sodium and potassium hydroxide (NaOH, KOH) are combined with silica (SiO_2) and alumina (Al_2O_3) – rich materials, such as fly ashes, slags and metakaolin, all of which presenting great binding properties (HEAH *et al.*, 2013). The main advantages of AAM over PC-based materials are their high chemical durability, great mechanical strength and lower environmental impact (PACHECO-TORGAL *et al.*, 2008B).

On the other hand, one important disadvantage of alkali-activated pastes, mortars and concretes is the early shrinkage. The shrinkage mechanism is basically an intrinsic property of the alkali-activated materials, which is not necessarily related to external actions. Shrinkage is also a big concern since it is probably the most common cause of cracking, which limits the employment of AAM in several applications (WALLAH & HARDJITO, 2015). One possible way to overcome this issue is the addition of fibers into the alkali-activated matrices (BARICEVIC *et al.*, 2015).

The investigation of AAM as repair materials for concrete structures is quite new; their compatibility, adhesion and durability need to be addressed, so that AAM may be employed as patch repairs in the near future.

1.1.OBJECTIVES

This research aims to develop alternative repair mortars for concrete structures by assessing the compatibility and the adhesion between alkali-activated mortars and a PC concrete substrate. The alkali-activated mortars will be obtained by partial substitution of metakaolin with blast furnace slag, changing the composition of the matrices (in terms of $[\text{SiO}_2] / [\text{Al}_2\text{O}_3]$ and $[\text{H}_2\text{O}] / [\text{Na}_2\text{O}]$ molar ratios). The specific objectives are:

- Pre-select alkali-activated mortars based on their mechanical behavior (compressive strength and modulus of elasticity);
- Assess the substrate-repair adhesion by performing pull-off testing and evaluate the crack propagation and delamination using four-point bending tests;
- Evaluate the physical properties (water absorption, apparent porosity and apparent density) of the alkali-activated mortars.

2. LITERATURE REVIEW

2.1. ALKALI-ACTIVATED MATERIALS

Alkali-activated materials (AAM) have been widely discussed, studied and promoted as greener binders for sustainable constructions. Those materials may be produced from a wide range of aluminosilicate (called as “precursor”) under alkaline conditions (induced by the “alkali activator”) to produce a hardened component (PROVIS, 2017).

The first synthesis of construction materials with alkaline activation was carried out in 1940 when Purdon studied the activation of a combination of high-calcium blast furnace slags. Almost two decades later, Glukhovsky proposed a general mechanism for alkaline activation of materials containing reactive silica and alumina, which is the first theoretical basis for the development of alkaline cements (PACHECO-TORGAL *et al.*, 2015).

Relevant changes concerning the chemistry of alkaline activation took place in the 1970’s. The researcher Joseph Davidovits created the term “geopolymer” to designate inorganic aluminosilicates subjected to alkaline activation similar to Glukhovsky model; he also patented several geopolymer formulations. More recently (in the 2000’s) valuable studies from Palomo (1999), Puertas (2000), Bakharev (2001-2002), Duxson (2007) and Provis and van Deventer (2009), contributed to the development of AAM (PACHECO-TORGAL *et al.*, 2015). Nowadays studies have been reported all over the world including developing countries in Latin America and Asia (PROVIS & VAN DEVENTER, 2014).

A very wide range of natural raw materials, industrial wastes and recycled aluminosilicates can be used as alkaline cement precursors: pozzolans, blast furnace slag (BFS), metakaolin (MK), pulverized fly ash (PFA), glass waste and the combinations of two or more of these materials (PACHECO-TORGAL *et al.*, 2015). AAM are cementitious materials resulted from the alkaline attack of amorphous aluminosilicates mixed with an alkaline activator (mostly sodium or potassium hydroxides and silicates) (PROVIS, 2017).

According to Provis and van Deventer (2014) there are different types of alkali-activated systems that must be distinguished:

- high-calcium alkali-activated systems, most of which are based on metallurgical slags;
- low-calcium alkali-activated systems, most of which are based on alkali aluminosilicates (metakaolin, for example) and including the free-calcium systems known as “geopolymers”, and;
- intermediate systems between calcium-based and aluminosilicate-based precursors, which result from their blend.

Figure 1 shows a schematic representation of those systems, as well as the comparison with Portland cement and calcium sulfoaluminate cements' chemistry.

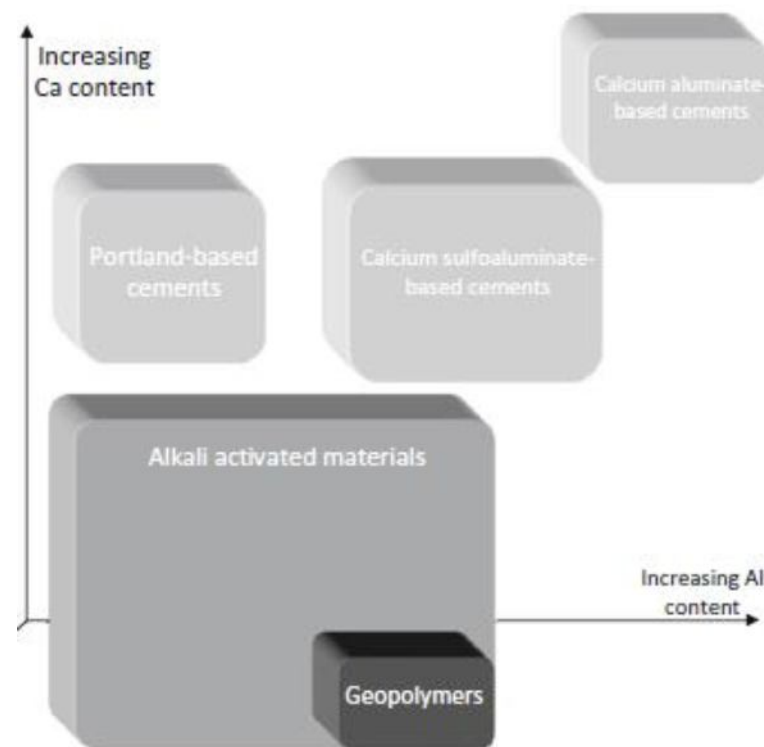


Figure 1 – Classification of AAM's and comparisons concerning chemistry (PROVIS & VAN DEVENTER, 2014)

It is essential to classify these systems according to the type of gel that controls the structure. Figure 2 shows this distinction processes mainly on the basis of the calcium content; the reaction products are either an alkali aluminosilicate-type gel (N-A-S-(H)) with approximated structure of $x\text{Na}_2\text{O} \cdot y\text{Al}_2\text{O}_3 \cdot w\text{SiO}_2 \cdot z\text{H}_2\text{O}$ or a calcium (alumino)silicate hydrate-type gel (C-A-S-H) with approximated structure of $x\text{Ca}_2\text{O} \cdot y\text{Al}_2\text{O}_3 \cdot w\text{SiO}_2 \cdot z\text{H}_2\text{O}$; in both cases x , y , w and z vary along the microstructure (PROVIS & BERNAL, 2014B).

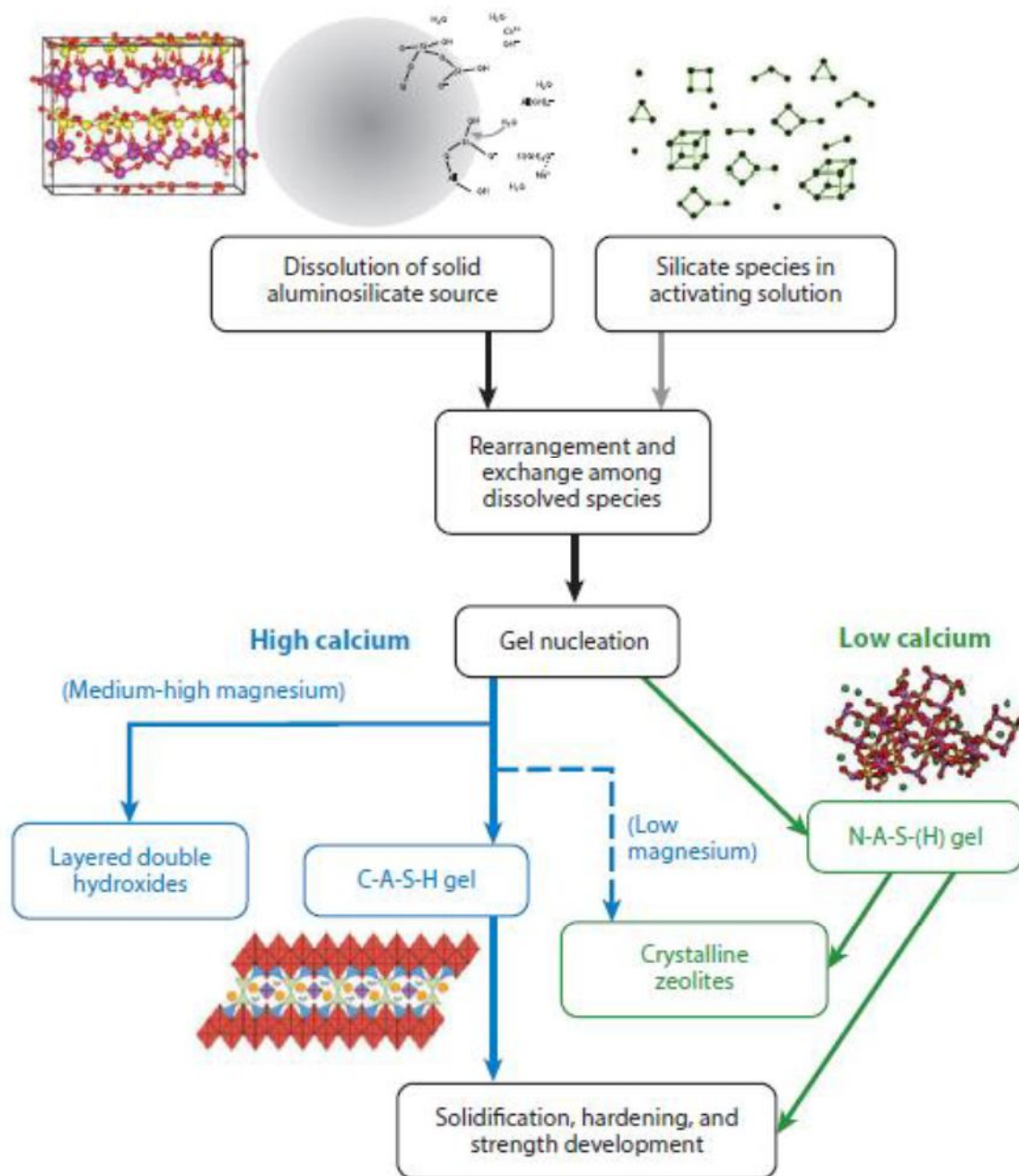


Figure 2 – Process and reaction products of different type activation (PROVIS & BERNAL, 2014B)

2.1.1. High calcium alkali-activated materials

The material most commonly used to produce high-calcium alkali-activated components is blast furnace slag (BFS). BFS is a vitreous steel industry by-product formed when the oxides present in the iron ore as impurities (SiO_2 and Al_2O_3) are combined with the basic oxides present in the limestone or dolomite (CaO and MgO) during the smelting and cooling process of iron slag. It's majority components are CaO (35-40%), SiO_2 (25-35%), Al_2O_3 (5-15%) and MgO (5-10%), while minor compounds include Fe_2O_3 , MnO and K_2O with percentages of under 1% (GARCIA-LODEIRO *et al.*, 2015).

According to the literature, some properties are required for the slag to be suitable for use in activated slag cements, such as: (i) must be granulated; (ii) have a vitreous phase content of 85-95%; (iii) have structural disorder; (iv) have a CaO/SiO_2 ratio of >1 ; and (v) must be ground to a specific surface of 400-600 m^2/kg (FERNÁNDEZ-JIMÉNEZ *et al.*, 1999; GARCIA-LODEIRO *et al.*, 2015).

The structure and composition of the C-A-S-H gel produced is directly dependent on the nature and amount of the activator used. The gel formed in a hydroxide-activated BFS presents a higher Ca/Si ratio and a more ordered and crystalline structure than in a silicate-activated BFS binder (BERNAL *et al.*, 2014). During the mix process the BFS will react very slowly with water only to form a hardened binder, so the key role of the alkali activator is to accelerate this reaction, allowing the material to harden and develop strength within hours after casting (PROVIS & BERNAL, 2014B).

The reaction products from Portland cement hydration may be similar to those of high-calcium AAM hydration. In the first, the hydration process gives a C-S-H type gel as the mayor product and secondary products as portlandite, ettringite and calcium monosulfoaluminate. On the alkaline reaction the main product is a C-A-S-H gel, slightly different from the Portland cement hydration, and secondary products that depends on the activator used, calcium source and composition and curing conditions, among others (GARCIA-LODEIRO *et al.*, 2015).

Besides BFS there are a few other high-calcium materials that can be used as precursors for alkaline activation, such as others steel slag, phosphorus slag, others metallurgical slags (copper slag, nickel slag, Cu-Ni slag and others) and bottom and waste incineration ashes (BERNAL *et al.*, 2014).

2.1.2. Low-calcium and calcium-free alkali-activated materials

The beginning of development of low-calcium (including calcium-free) alkali-activated binders took place in the 70's with Davidovits work in France (PROVIS, FERNÁNDEZ-JIMÉNEZ, *et al.*, 2014). The most commonly applied materials for alkaline activation of low-calcium systems are pulverized fly ash (PFA) and metakaolin (MK). The low calcium content in these two raw materials allows for the production of alkali-activated materials with high mechanical strength and good chemical durability (GARCIA-LODEIRO *et al.*, 2015).

The low-calcium alkali-activated system is structurally disordered and its main product is a N-A-S-(H) gel as shown in Figure 3 (PROVIS & BERNAL, 2014B). Its structure is constituted by a three-dimensional network where silicon and aluminium atoms alternate in a tetrahedral coordination, sharing the oxygen atoms. Three basic structures are formed during the activation: Poly(sialate), Poly(sialate-siloxo) and Poly(sialate-disiloxo) according to Figure 4. Positive ions (Na^+ , K^+ , Li^+ , Ca^{++} , Ba^{++} , NH_4^+ , H_3O^+) must be present to keep the equilibrium within the chain due to the deficit generated by the combination between Al^{3+} and Si^{4+} with O^{2-} ions (DAVIDOVITS, 1994).

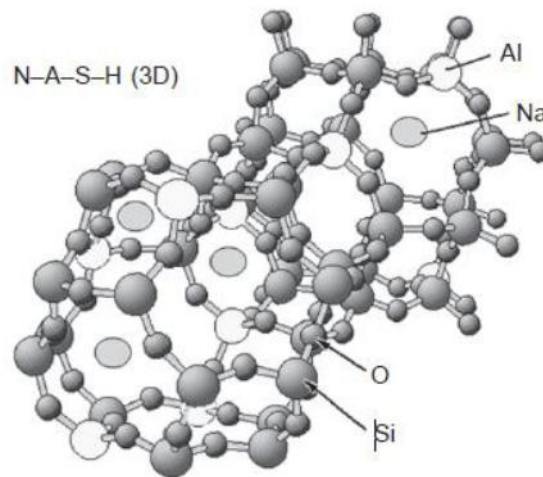


Figure 3 – View of the three-dimensional structure of a N-A-S-H gel (GARCIA-LODEIRO *et al.*, 2015)

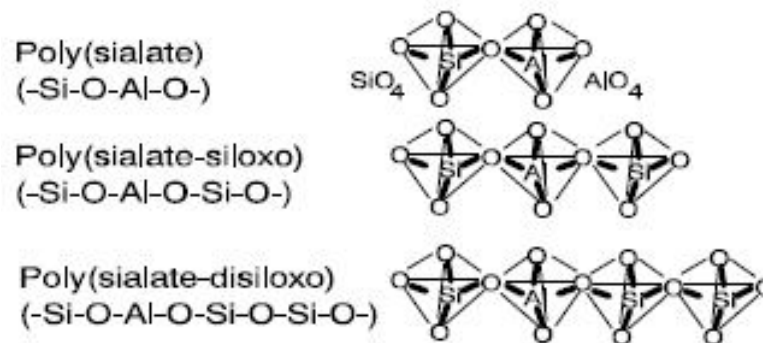


Figure 4 – Types of gel structures (DAVIDOVITS, 1994)

The term “geopolymer” has been employed to designate a wide range of alkali-activated binders (most commonly to low-calcium or calcium-free systems); nowadays, it is restricted to calcium-free systems only (PROVIS, FERNÁNDEZ-JIMÉNEZ, *et al.*, 2014).

As mentioned before, one of the main raw materials used as precursor for the geopolymers is metakaolin. MK is a pozzolanic material generated as a result of kaolinite clay calcination at temperatures ranging from 500 to 800 °C (Figure 5),

process which doesn't generate CO_2 to the atmosphere (GARCIA-LODEIRO *et al.*, 2015). The feasibility of MK as an aluminosilicate source depends deeply on the particle size, purity, and crystallinity of the initial kaolinite, properties that influence its reactivity. The typical MK composition is 50-55% of SiO_2 and 40-45% of Al_2O_3 ; however, it may contain others compounds in small quantities, such as Fe_2O_3 , TiO_2 , CaO , MgO and Na_2O (LI *et al.*, 2010).

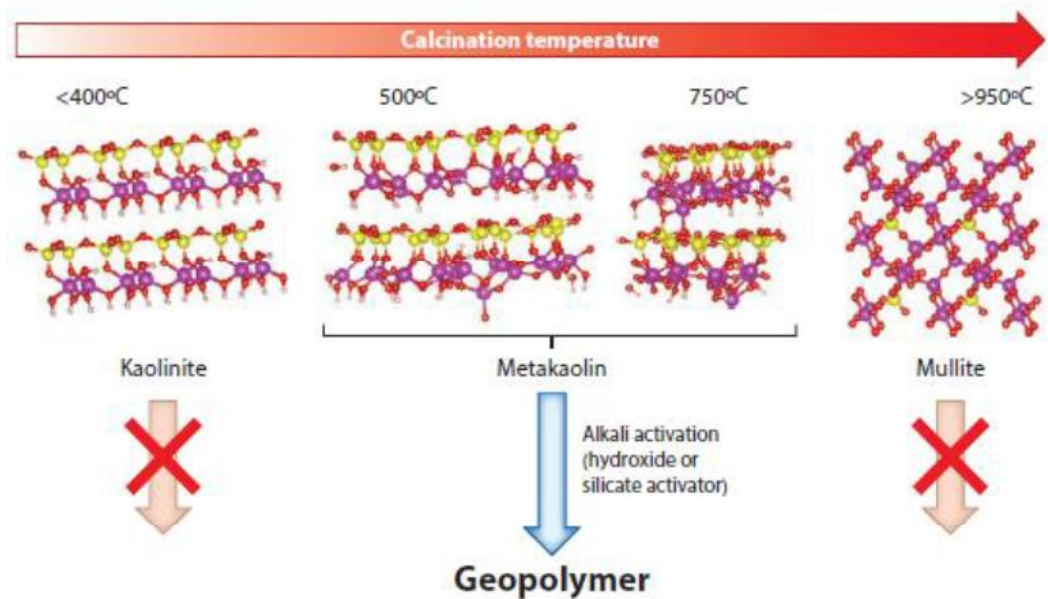


Figure 5 – Pathways for the conversion of kaolinite (PROVIS & BERNAL, 2014B)

2.1.3. Blended alkali-activated systems

Over the past years the motivation for studies focused on blended systems has considerably increased. The reason for that is the need for durable, high-performance, low- CO_2 alternative binder systems. These binders are expected to provide a stable synergy between the reaction products, C-A-S-H gel of slags systems and N-A-S-(H) gel of MK/PFA systems (PROVIS & BERNAL, 2014A).

It is known that C-A-S-H-type gels provide a great chemical binding reducing permeability, whereas N-A-S-(H)-type gels can provide binders with excellent chemical and thermal resistance. Therefore, the coexistence of these two types of gel can contribute to the material performance (PROVIS & BERNAL, 2014B). The gel coexistence requires a pH that is not high enough to cause the reactive calcium precipitation as portlandite. Therefore, the alkali activation of MK or PFA with slags is highly dependent on the alkalinity of the activator and the ratio of blending the solid precursors (PACHECO-TORGAL *et al.*, 2015).

The most commonly blended alkali-activated system studied is the MK-BFS system. Buchwald *et al.* (2007) studied the chemical interaction of a combination of BFS-MK activated by a sodium hydroxide solution. Nuclear magnetic resonance spectroscopy (NMR) with XRD and DTA/TG were used to investigate whether both raw materials react separately or there was a chemical interaction between them. They concluded that both reaction products can coexist and there is a small interaction resulting in a better strength performance (BUCHWALD *et al.*, 2007). It is also known that the alkaline activation of blended systems rich in calcium (e.g. MK-BFS) accelerate the condensation reaction (BUCHWALD *et al.*, 2009).

Some studies have addressed the influence of the activator concentration and mix parameters (MK to BFS ratio) on the alkali-activated pastes, focusing on the structure and fresh, mechanical, physical and thermal performance (BERNAL *et al.*, 2011; BERNAL *et al.*, 2013; BORGES *et al.*, 2016; SAMSON *et al.*, 2017). According to these studies the inclusion of BFS in MK-based matrices improves the performance when exposed to high temperatures, reduces the overall porosity due to the matrix densification and improves the fresh properties and the compressive strength.

However, some others blended systems have been also studied (PUERTAS & FERNÁNDEZ-JIMÉNEZ, 2003; BERNAL *et al.*, 2012; BIGNOZZI *et al.*, 2013; WANG *et al.*, 2015; SAMSON *et al.*, 2017). Puertas and Fernández-Jiménez (2003) proved the coexistence of two different reaction products within PFA/BFS 50/50 (wt.%) matrix: (i) a calcium silicate hydrate rich in Al, containing Na in its structure and (ii) an alkaline aluminosilicate hydrate with a 3D structure, resulting from the fly ash activation. Wang *et al.* (2015) and Samson *et al.* (2017) also studied a PFA/BFS system and found that the fresh properties and the compressive strength were improved with the PFA replacement by BFS.

Bignozzi *et al.* (2013) studied a blended system of MK and ladle slag (deriving from refining process of steel produced by arc electric). These authors discovered that even when the ladle slag does not react completely; it participates in the consolidation process of the matrix. They also suggested that the slag strongly influences the porosity of the matrix and allows the formation of C-S-H, 3D aluminosilicate network and a C-A-S-H gel.

2.2. CONCRETE STRUCTURAL REPAIR

Concrete repair is a complex task requiring a special knowledge involving technical building regulations and standards, several construction materials, deterioration mechanism, diagnosis, repair principles and methods, repair materials, execution of repair works, inspections, monitoring and maintenance (RAUPACH & BUTTNER, 2014). In the recent years the repair of concrete structures has become a worldwide activity representing a multimillionaire opportunity for the construction industry (PACHECO-TORGAL *et al.*, 2012).

The estimated cost for maintenance of all types of buildings is in the trillion dollar house worldwide every year and a significant part of this amount is spent on repair and protection of concrete structures. This huge opportunity of market directly influence the industry interest and the development of new materials, principles and techniques for the repair of concrete structures (RAUPACH & BUTTNER, 2014).

Therefore, the extensive development of new methods and materials for concrete structural repair has led to the need for standard and regulations. As a reference for this work, the European Standard EN 1504 - Protection and Repair of Concrete will be discussed hereafter.

2.2.1. European Standard - EN 1504

The European Standard EN 1504 provides a systematic approach from the principles and methods of repair and protection of concrete structures to the selection of suitable products and quality control. It is divided in ten standards series beginning with definitions, passing through the products, it's principles for using, quality control of the products and of the repair work and finishing with the site application (RAUPACH & BUTTNER, 2014).

According to the EN 1504 (2005) the repair project follows a logical sequence of action that must be taken to execute the repair work of the damaged structure. This logical sequence is dominated by engineering aspects and is summarized in Figure 6.

The first thing to assess during a repair process work is to determine the cause or causes of damage and understand the process that leads to this defect, with attention to distinguish the defects in concrete from those caused by reinforcement corrosion. As shown in Figure 7, damages in concrete may be induced by mechanical, chemical or physical attack or by fire. In the cases of reinforcement

corrosion, the damage may be due to carbonation or corrosive contaminants (RAUPACH & BUTTNER, 2014).

PROJECT PHASES

Information about the Structure	Process of Assessment	Management Strategy	Design of Repair Work	Repair Work	Acceptance of Repair Work
---------------------------------	-----------------------	---------------------	-----------------------	-------------	---------------------------

Basis considerations and actions

Conditions and history of structure	Defects and their classification and causes	Options	Intended use of products	Choice and use of products and systems and methods and equipment to be used	Acceptance testing
Documentation	Safety/ structural appraisal before protection and repair	Principles	Requirements - substrate - products - work	Tests of quality control	Remedial works
Previous repair and maintenance		Methods	Specifications	Health and safety	Documentation
		Safety/ structural appraisal during protection and repair	Drawings		
			Safety/ structural appraisal after protection and repair		

Figure 6 – Logical sequence (phases) of repair projects (RAUPACH & BUTTNER, 2014)

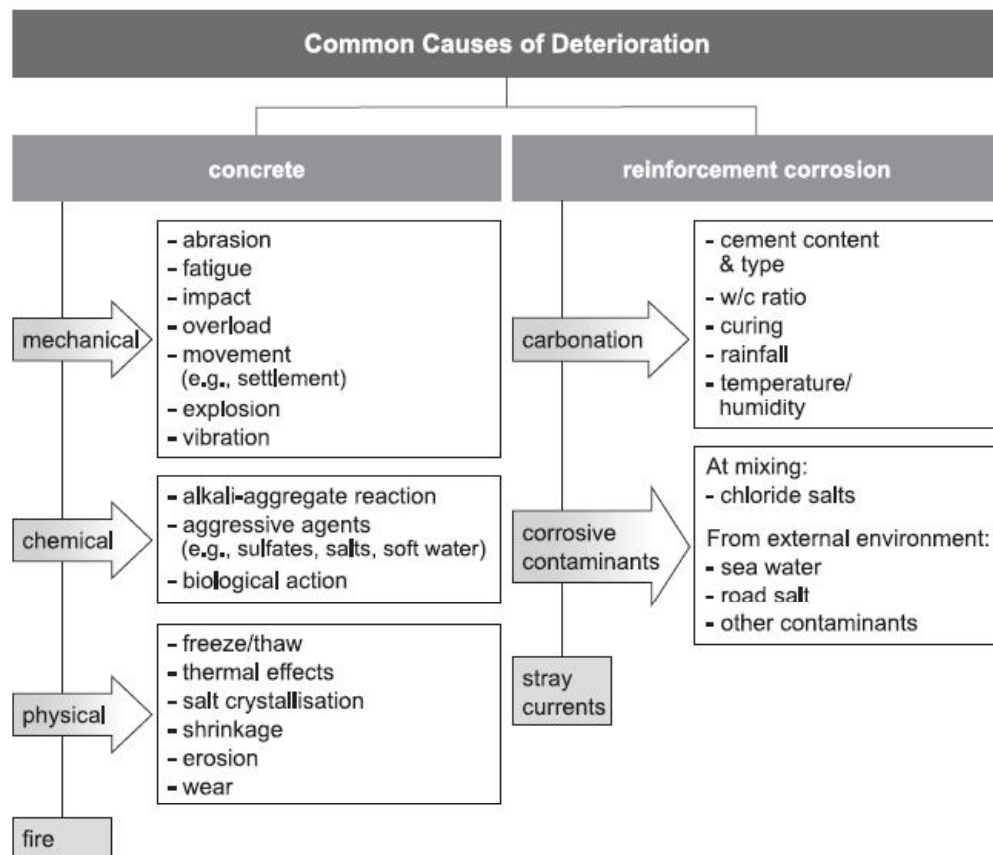


Figure 7 – Common causes of damages in structures (RAUPACH & BUTTNER, 2014)

An assessment of the structure must be carried out following the understanding of the damage process; it must include some important topics (not limited to), such as: (i) visible condition of the existing structure; (ii) testing to determine the real condition of the structure; (iii) the environment, including exposure to contamination; (iv) the history of the concrete structure; (v) the service conditions; and (vi) future requirements (EN, 2005).

According to the EN 1504 (2005), for most of the repair methods the first step is the surface preparation. It is considered one of the most important steps to accomplish a successful concrete repair. The standard presents an overview of the most commonly used methods for surface preparation. Then, the correct repair material is selected based on the substrate conditions, according to the logical sequence of repair projects presented by the EN 1504.

2.2.2. Conventional materials as repair mortars

In general, the conventional materials used to repair concrete structures are cement mortar/concrete, sprayed cement mortar/concrete, polymer-modified mortar/concrete and polymer mortars.

The thickness of the repair patch is a crucial aspect to choose which type of repair material to use. Cast or sprayed concrete are usually used for larger thickness, at least 30 mm for sprayed concrete and 50 mm for cast concrete. Cement mortars are the most indicated in the case of thinner layers repair, with thickness between 20 mm and 40 mm (RAUPACH & BUTTNER, 2014).

Besides the thickness of the repair, the orientation of application also contributes to the material selection. Cast concrete is only used for repair of horizontal or vertical (formwork required) surfaces; in contrary, sprayed concrete can also be used for overhead surfaces. In the case of cement mortars the application can be carried out either by casting *in situ* with formwork or by spraying. In the latter, polymers are added into the mix and those materials change their category to polymer-modified mortars (RAUPACH & BUTTNER, 2014).

Ordinary and rapid-hardening Portland cement are the types of cement most frequently used in repair works. However, the repair mortar may be composed with the same cement type of the original structure, e.g. in cases where the existing structure was built with sulphate-resisting Portland cement. High-alumina cement is sometimes used when fast strength development is required, but this is a typical non-

structural application such as temporary repairs where long-term durability it is not required (MASSON & ALLEN, 1993).

For polymer-modified mortars, the difference in the mortar composition is the polymer content, which is usually between 0.5% and 5%, and limited to a maximum of 10% (volume fraction). The main reasons for adding polymers are: (i) to increase the surface adhesion; (ii) to increase the water retention; (iii) to enhance workability; (iv) to increase the bending and tension strength, and (v) to reduce the Young's modulus when necessary. Several types of polymers have been used into modified cementitious systems, including polyvinyl acetates, styrene butadiene, polyvinylidene dichloride, acrylics and modified acrylics (SHAW, 1993).

In contrast to these previous types of repair materials, polymer mortars do not contain Portland cement as binder; polymers are the only reactive materials. These mortars should be used only if fast-drying patch is required, no curing treatment is possible or for extremely low thickness (less than 12 mm). Epoxy resins are the most commonly used, but polyester and acrylic resins are also used when rapid strength development is required (SHAW, 1993; RAUPACH & BUTTNER, 2014).

2.2.3. Alkali-activated materials as potential repair materials

So far, most used patch repair mortars fall into two categories, the mortars based on inorganic binders (Portland cement) and those based on organic binders (polymers). Recent investigations, however, reveal a third category of mortars with high potential to be used in the field of concrete repair, i.e. the alkali-activated based mortars. The lack of studies in alkali-activated field addressed to rehabilitation of concrete structures can be related to the fact that many alkali-activated research groups belong to the materials science field and not specifically to civil engineering (PACHECO-TORGAL *et al.*, 2012).

Nevertheless, a few studies have been carried out assessing the performance of alkali-activated mortars as repair materials for deteriorated concrete structures. A metakaolin-based mortar with steel slag proved to have better repair characteristics (compressive strength, bond strength and abrasion resistance) than cement-based mortar (HU *et al.*, 2008). Zhang and Wang (2015) aimed to develop a new protective coating of OPC concrete structures exposed to marine conditions based on alkali-activated MK mortar. The good bonding (up to 3 MPa in tension and 20 MPa in slant shear test) between both materials and the excellent corrosion resistance of the

alkali-activated coating provided a durable effective protection of the OPC concrete (ZHANG & WANG, 2015).

A new pavement repair material was investigated by comparing some characteristics (effect of curing time, bond strength by splitting tensile test and slant shear test and durability) of conventional repair materials with a metakaolin-based geopolymer (ALANAZI *et al.*, 2016). These authors founded that the bond strength of the suggested geopolymer mortar was higher than that of OPC and greatly affected by the curing time and temperature; the authors also suggested that in the first 24 hours of curing the geopolymer develops a low compressive strength, which has a negative influence on the bond with the substrate.

Zhang *et al* (2015) also studied the effect of curing temperature on AAM repair materials; they assessed the bond strength of eighteen different metakaolin/fly ash-based geopolymers with addition of short carbon and basalt fibers through double shear test in different temperatures (20-300°C). The geopolymers presented lower bond strength than the conventional epoxy resin at room temperature; the addition of fibers did not influence the bond. At higher temperatures (100-300°C) the geopolymers presented much higher bond strength and the use of fibers greatly improved the bond strength throughout crack control (ZHANG *et al.*, 2015).

Following the EN 1504 series requirements, three different alkali-activated mortars (based on fly ash (FA), ground blast furnace slag (BFS) and metakaolin (MK)) were investigated regarding their suitability for concrete repair use (KRAMAR *et al.*, 2016). Several properties were studied, such as workability, compressive and flexural strength, modulus of elasticity, bond strength by pull-off, shrinkage and expansion and capillarity absorption resistance. The BFS-based activated mortar delaminated from the substrate, therefore unsuitable for application as patch repair. The mechanical properties of both MK and FA-based activated mortars complied with EN 1504 values but the shrinkage of the FA mortar was much higher than the MK mortar. High capillarity absorption coefficient were found for all mortars, values which were far beyond the accepted for repair materials. The overall characterization indicated the MK mortar as the most suitable, but major improvements on durability properties were needed (KRAMAR *et al.*, 2016).

Zanotti *et al* (2017) studied the bond strength between a concrete substrate and a metakaolin-based repair mortar, considering the curing time effect (20°C and 45°C) and PVA fiber reinforcement content (0%, 0.5% and 1%). A non-standard slant shear

test was carried out to evaluate the bond strength and the interfacial cohesion between both materials. Ambient cured metakaolin mortar presented a significant early-age cracking along the surface and along the interface, affecting the cohesion between materials. The early-age cracking was prevented by the heat curing, increasing the bond strength of the repair mortar. Overall the authors concluded that the cohesion is significantly improved with the addition of fibers, notably for 0.5% vol. PVA (65% increase in cohesion for heat cured and 204% for ambient cured samples) (ZANOTTI *et al.*, 2017).

2.3. SUBSTRATE-REPAIR COMPATIBILITY

The compatibility of the repair material with the existing substrate is an important consideration in the repair industry, as it implies durability and adequate load capacity of repairs in structural cases. The application of repair materials and systems requires dimensional compatibility, bond compatibility and durability, structural and mechanical compatibility and some compatible physical characteristics between the new materials (repair) and the old part (substrate) (MORGAN, 1996).

Compatibility can be defined as a balance of physical, chemical, electrochemical as well as dimensional properties between a repair material and the existing substrate. This compatibility will guarantee that the repair performs its function over a long period of time without failure or deterioration (EMMONS *et al.*, 1993). Figure 8 summarizes several factors that influence the compatibility of repair materials.

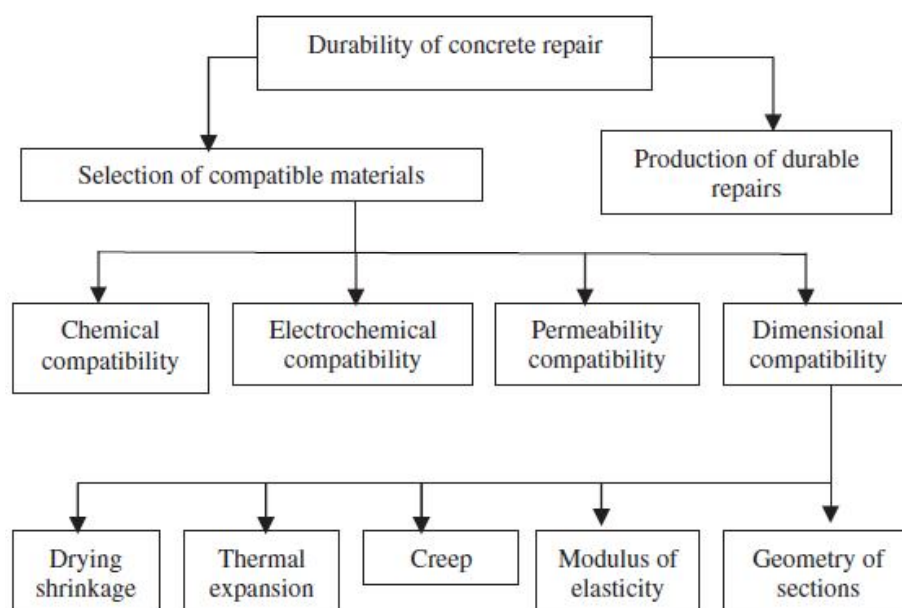


Figure 8 – Factors that influence the durability of repair materials (EMMONS *et al.*, 1993)

The most important consideration of all is probably the dimensional compatibility, which will determinate whether the repair area will withstand load and volume variations without loss of bond strength and consequent delamination (MORGAN, 1996). Pacheco-Torgal *et al* (2012) discussed some of the general requisites for repair mortars concerning structural compatibility, requirements which were first presented by Emmons *et al* in 1993 in their work about durable concrete repairs (Table 1).

Table 1 – Structural compatibility between substrate and repair mortars

Properties	Relation between the repair mortar (Rp) and the concrete substrate (Cs)
Mechanical Strength	$R_p \geq C_s$
Modulus in compression	$R_p \sim C_s$
Poisson ratio	Dependent on modulus
Coefficient of thermal expansion	$R_p \sim C_s$
Adhesion in tension and in shear	$R_p \geq C_s$
Curing and long term shrinkage resistance	$R_p \geq C_s$
Strain capacity	$R_p \geq C_s$
Fatigue performance	$R_p \geq C_s$

Adapted from Pacheco-Torgal *et al.*, 2012

The main causes of delamination or de-bonding are excessive (i) shrinkage strains; (ii) expansions; and (iii) thermal expansions and shrinkage resulting in cracks development. Other parameters can also influence dimensional compatibility such as size, shape and thickness of the repaired area, the amount of reinforcement or anchorage (if any), modulus of elasticity and strain capacity (MAILVAGANAM, 1992; MAROSSZEKY, 1992; MORGAN, 1996).

According to Morgan (1996) the substrate preparation is the most important requirement of a successful repair. The correct preparation of the substrate surface may improve the bond compatibility and the bond durability, thus preventing the repair failure. The preparation methodology varies for different construction applications, taking always into consideration the adequate surface roughness.

Overall repair mortars are likely to be compatible if they present appropriate modulus of elasticity and low volume change capacity, thus preventing cracking from excessive shrinkage and expansion or interfacial stresses that lead to bond failure (EMMONS *et al.*, 1993; MORGAN, 1996).

2.4. SUBSTRATE-REPAIR ADHESION

The substrate-repair adhesion usually represents a weak link in the repaired structure. The bond strength mainly depends on the stress applied: shear, tension or combined shear and normal stresses. In tension, bond is mostly affected by the adhesion of roughness (change in contact area). In shear the two main contributions are cohesion and friction, with cohesion being mostly affected by adhesion and interlock. Adhesion depends on bonding agent (if any), specimen age, cleanness, moisture and roughness of the substrate surface (MOMAYEZ *et al.*, 2005).

Bond compatibility and durability are important aspects for the substrate-repair adhesion. The bond compatibility is the satisfactory development of bond strength between the substrate and the repair, and the bond durability is the maintenance of this bond over time. Several factors, such shrinkage, volume changes, different types of load or any kind of direct stress, can affect the bond interface (MORGAN, 1996).

Numerous types of tests are available to measure and evaluate the bond strength between the old concrete substrate and the new repair material. The existing tests can be divided into some categories, such as: (i) bond measured under tension stress; (ii) bond measured under shear stress and, (iii) bond measured under combination of shear and compression stress (MOMAYEZ *et al.*, 2005).

As reference for this work two different types of evaluation will be discussed, a tension stress situation (pull-off test) and a second one to evaluate the interfacial crack growth resistance (also known as crack trapping mechanism).

2.4.1. Bond strength by pull-off test - British Standard (BS EN 1542)

The British Standard 1542 describes a method for measuring the tensile bond strength of repair products and systems by direct pull-off test using a dolly bonded to the surface of the repair. This standard provisions are applicable to repair systems with a maximum thickness of 50 mm (EN, 1999)

Some of the equipment needed for the method are: (i) circular dollies that should have a diameter of 50 mm and must ensure that the load can be applied normal to the surface, without creating bending or shear forces in this area; (ii) a diamond core drill to enable drilling a cylinder through the repair materials; (iii) a pull off test equipment, and; (iv) concrete specimens with rough surface (EN, 1999).

The repair material must be applied in the vertical position on the concrete substrate. The specimen prepared should be stored in the vertical position for three

days under the laboratory conditions of temperature and humidity and then be laid horizontal to keep curing until a determined period. A minimum of one test specimen (one panel) is required for each type of repair material, from which five bond tests will be carried out (EN, 1999). Figure 9 presents an example of a schematic plan of a 300 x 300 x 100 mm specimen showing the dolly distribution.

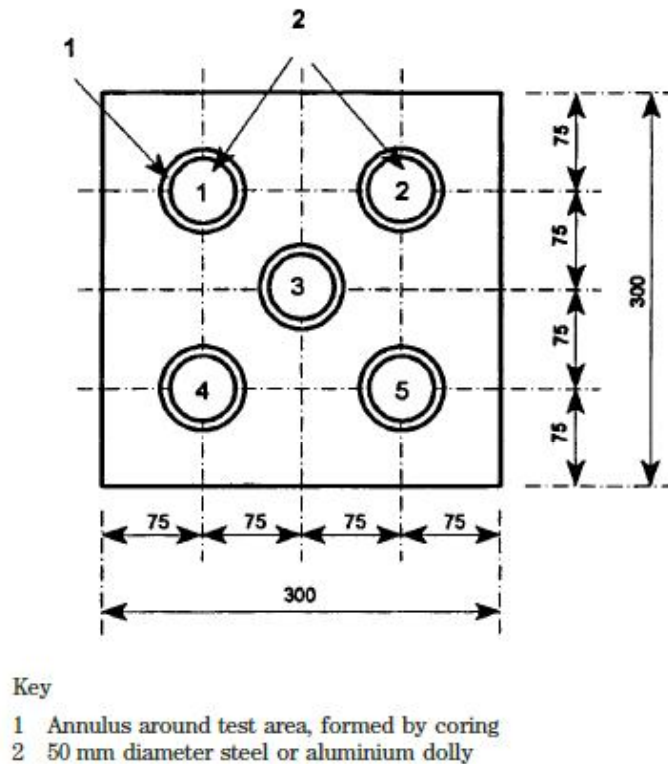


Figure 9 – Scheme with the dolly distribution (EN, 1999)

The test is carried out after the desired curing period, following the steps of core drilling, application of the dolly, setting of the pull-off equipment and load application (rate of 0.05 MPa/s). The value of the bond strength is obtained within the equipment and a visual evaluation is used to determinate the type of failure of the specimen (EN, 1999).

According to EN 1504-3 (2005) four mortar classes are defined considering application and the adhesion bond: R1 and R2 for non-structural mortar and R3 and R4 for structural mortar (Table 2).

Table 2 – Standard adhesion bond requirement

	R1	R2	R3	R4
Adhesion bond (MPa)	≥ 0.8	≥ 0.8	≥ 1.5	≥ 2.0

2.4.2. Crack Trapping Mechanism Test

Another important parameter for durable repair systems is the interfacial fracture toughness. The problems in repaired structures are related in most of the cases to cracking along the interface or kinking of cracks out the interface. In both cases, the crack will propagate along the least resistance part (the substrate, the repair or the interface between them) (LI *et al.*, 1995).

The interfacial fracture toughness calculated from a four-point bending test is a parameter which is capable of predicting repair system performance associated with interface crack evaluation. This parameter can predict whether an interface crack will propagate along the interface (situation when delamination occurs) or will deviate from the interface. Besides, such test also help assess the load magnitude necessary to initiate the crack (LIM & LI, 1997).

One technique to overcome this failure problem in repair systems is the interface crack trapping mechanism. The trapping mechanism consist on the ability of a high performing material to arrest (trap) a crack that deviate, so that damage can propagate in another region (interfacial or not) and additional toughness at the interfacial region is achieved (LIM & LI, 1997).

To assess its mechanism, the specimens are designed to include a defect in an interfacial crack form between the repair material and the concrete substrate and also a joint in the substrate. Four-point bending test should be used to create a loading condition. Figure 10 shows the dimension of specimen and the loading configuration system (LIM & LI, 1997).

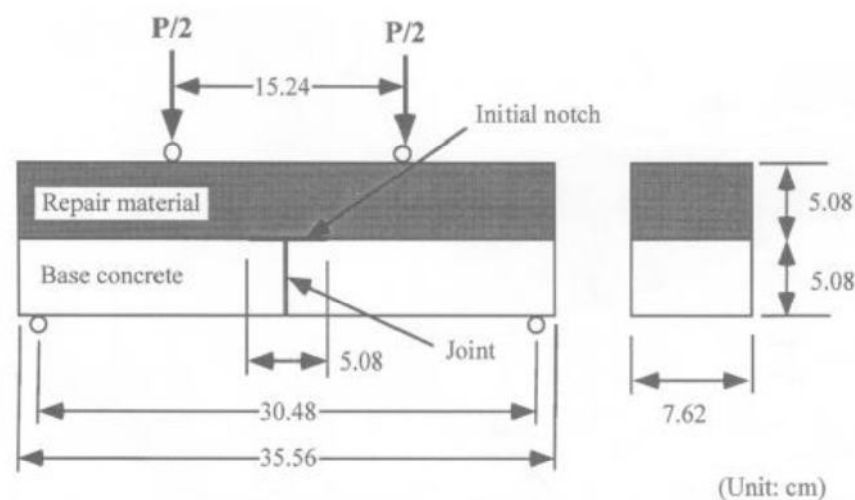


Figure 10 – Dimension of specimen and loading configuration for a crack trapping mechanism test (LIM & LI, 1997)

The conceptual trapping mechanism load-displacement relation is illustrated in Figure 11. This curve indicates how the crack behaves and develops during the load application, characterizing a process with a large amount of energy absorption associated with an extensive surface damage in the repair material without loss of load carrying capacity.

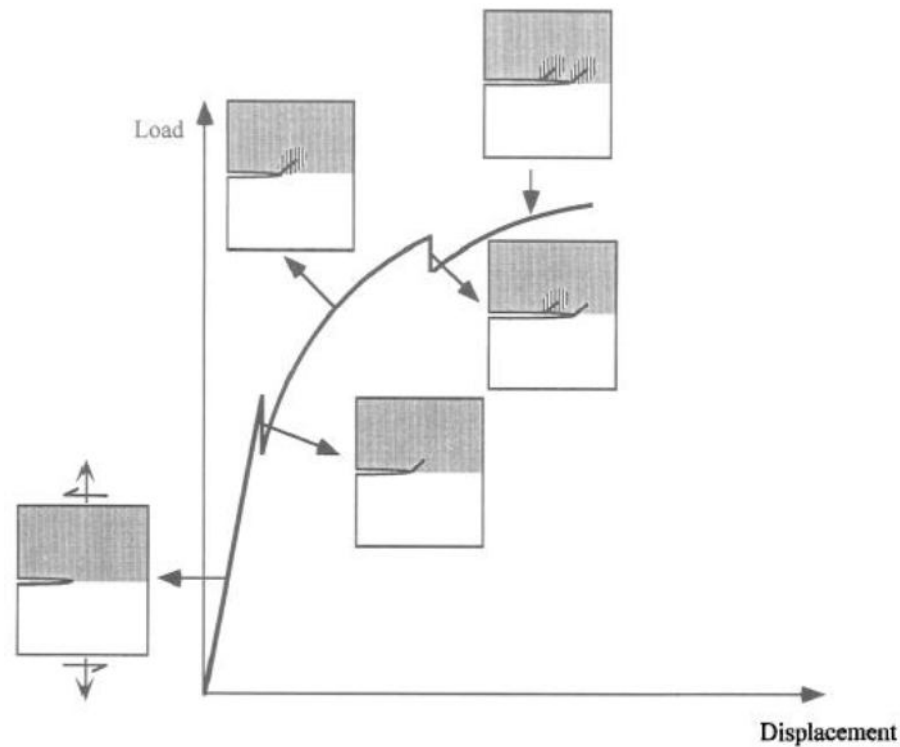


Figure 11 – Load-displacement curve (LIM & LI, 1997)

An interface analysis is carried out after the failure to determine the crack propagation pattern. If the repair material is brittle, the crack forms a surface spall. On the other hand, if the repair material has fracture resistance, the crack is “trapped” in the repair material and no more crack propagation occurs. This last is possible if the repair material is fiber reinforced (LIM & LI, 1997).

Therefore, this mechanism is an interesting analytical tool to evaluate the bond strength and the compatibility between the concrete substrate and the repair mortar, concerning crack propagation and delamination.

2.5. USE OF FIBERS IN STRUCTURAL REPAIR

The incorporation of fibers into concrete creates Fiber Reinforced Cementitious composites (FRCC). The fiber addition in general has significant influence on specific cement-based materials properties, specially tensile and flexural toughness and

energy absorption capacity through crack-bridging. The durability of these composites is also enhanced through crack control (AHMED, 2014).

Different types of fibers are available in the market, from steel and polymer to fibers produced from different recycled materials; a proper selection depends on their properties and target application. Cement composites with Polypropylene fibers are most frequently used due to their low cost, inert behavior in alkaline environment and relatively good dispersion in cement matrices (BARICEVIC *et al.*, 2015).

Several studies assessed the influence of PP fibers in the composites properties, such as: plastic shrinkage (NAAMAN *et al.*, 2005; BANTHIA & GUPTA, 2006; MYERS *et al.*, 2008; GHODDOUSI & JAVID, 2010), autogenous shrinkage (MYERS *et al.*, 2008; SAJE *et al.*, 2012), drying shrinkage (LAMOUR *et al.*, 2005; KUMAR *et al.*, 2013), restrained shrinkage (LAMOUR *et al.*, 2005; BANTHIA, 2010; IDEKER & BAÑUELOS, 2014), tensile strength (SONG *et al.*, 2005; GENCEL *et al.*, 2011; PATEL *et al.*, 2012), modulus of elasticity (BANTHIA, 2010) and compressive strength (BAYASI & ZENG, 1993; SEFEROVIĆ, 2002; SKAZLIĆ, 2003; KUMAR *et al.*, 2013).

The main contribution of PP fibers additions is their beneficial effect on autogenous, plastic and restrained shrinkage of cement composites, affecting thus its durability. It also contributes to the adhesion between the repair material and the repaired structure. Due to those characteristics they are often used in repair materials (BARICEVIC *et al.*, 2015).

There is a lack of studies in the literature regarding the use of fibers into alkali-activated material for structural repair purpose. Few studies, however, addressed the use of fiber-reinforced polymer sheets for repair and strengthening concrete structures (DAVIDOVITS *et al.*, 1998; DAVIDOVITS, 1999; KURTZ *et al.*, 1999; VASCONCELOS *et al.*, 2011; PACHECO-TORGAL *et al.*, 2012; MENNA *et al.*, 2013). The use of short fibers and their influence on crack control and on bond strength were studied by Zhang *et al.* (2015) and Zanotti *et al.* (2017) as presented at section 2.2.3.

3. METHODOLOGY

3.1. SCOPE OF THIS STUDY

The experimental program proposed in this dissertation is divided into three main parts: assessment of (i) compatibility; (ii) adhesion and (iii) physical properties. The characterization of the raw materials was carried beforehand.

The first phase focused on the structural requirements of AAM to act as repair materials, i.e. pre-selection of preliminary alkali-activated mortars based on their compressive strength and modulus of elasticity (21 formulations were narrowed down to 5).

The second phase concerned the adhesion evaluation between those two materials (repair mortar and PC substrate), determined by the pull-off testing and the crack trapping mechanism test (via four-point bending test).

The third phase was the physical evaluation of the repair mortars. The following tests were carried out: water absorption and apparent density and porosity. A flowchart of the experimental program is presented in Figure 12.

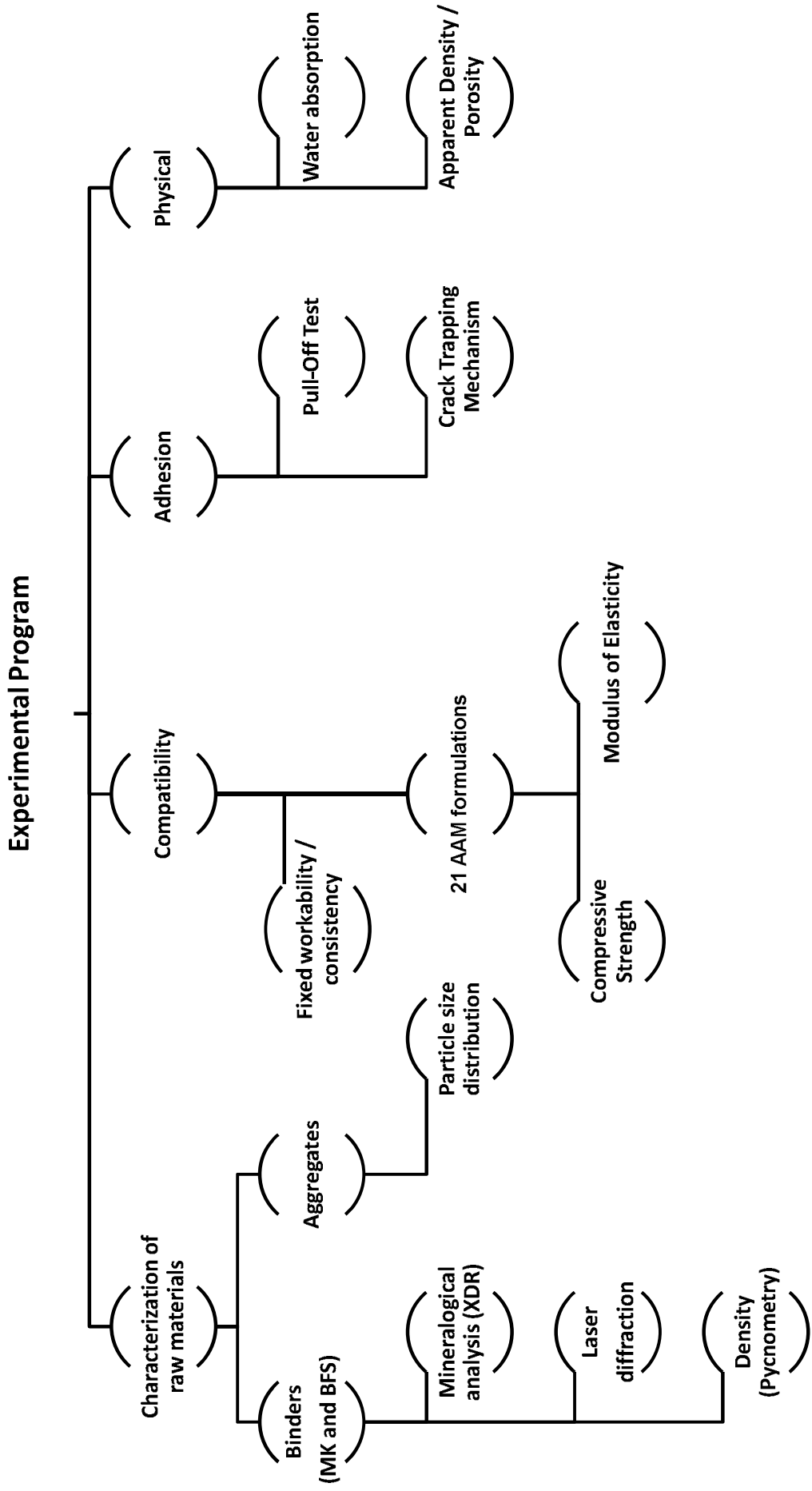


Figure 12 – Flowchart of the experimental program

3.2. MATERIAL AND METHODS

3.2.1. Materials

Two aluminosilicates were used as precursors to produce the alkali-activated repair mortars, i.e. metakaolin (MK) and blast furnace slag (BFS), supplied by Metacaulim do Brasil and by Mizu Cimentos Especiais, respectively. The alkali activator solution was composed of a mix of sodium hydroxide (NaOH) 50% vol. and sodium silicate (Na_2SiO_3) provided by Imperial Química and Getex, respectively.

The following tests were used to characterize the precursors (MK and BFS): (i) mineralogical analysis and amorphicity degree by X-Ray Diffraction (XRD); (ii) particle size distribution by laser diffraction and (iii) apparent density by Helium Pycnometry.

The XRD analysis was carried out at 1° per minute (step size of 0.02°) from $2\theta = 5^\circ$ to 80° using the XRD-7000 Shimadzu diffractometer (Figure 13) with copper radiation operating in 40 kV and 30 mA.



Figure 13 – Shimadzu XRD-7000 equipment

The particle size distribution was obtained by laser diffraction using the particle size analyser CILAS 1090 (Figure 14). The raw materials were dispersed in water and the parameters used were a disturbance of 1500 rpm, obscuration between 10% and 20%, ultrasound time of 2.5 min and dispersion time of 5 min.



Figure 14 – CILAS 1090 LASER particle size analyser

The apparent density was obtained by helium gas pycnometry using a Multipycnometer MVP-6DC from Quantachrome (Figure 15).



Figure 15 – Pycnometry equipment

The fine aggregate used to produce the alkali-activated mortars was a dolomite aggregate supplied by Dacapo Minasit. Three particle size envelopes were combined in defined proportions to obtain a mixture of aggregates with particle size distribution within the optimum envelope according to the Brazilian standard NBR 7211 (ABNT, 2009).

Short polypropylene fibers (PP) FibroMac 6 from Maccaferri do Brasil were used to reinforce the repair mortars. The PP fiber employed had diameter of $18\mu\text{m}$, length of 6 mm and a specific weight of 0.91 g/cm^3 .

A commercial structural mortar 240 from Vedacit was used as reference to compare its performance with the alkali-activated mortars. A rapid-hardening Portland cement (CPV ARI type) from Holcim Brasil was used to cast the concrete

substrate; natural river sand with fineness modulus of 2.19 was used as fine aggregate and gnaiss gravel (maximum size of 25 mm) as coarse aggregate for the PC concrete substrate. A surface setting time retarder RT-35 supplied by Dacapo Minasit was used (see section 3.2.2).

3.2.2. Concrete substrates preparation

3.2.2.1. Substrate for the pull-off test

C30 concrete class substrates (compressive strength of 30 MPa at 28 days) were cast using the following mix design (ACI method) 1: 2.46: 3.88 (cement : fine aggregate : coarse aggregate) and w/c ratio of 0.65. The mixture was batched in a 400L concrete tumble mixer. The concrete substrates were cast in timber formwork molds with dimensions of 40 x 40 x 08 cm (W x L x H). Cylindrical samples (10 x 20) cm were cast for mechanical evaluation to ensure that the mix design was correct.

A surface setting retarder (RT-35) was used to expose the aggregates and create a uniformly irregular surface with proper adhesion to receive the repair mortar according to the European standard of repair of concrete structures EN 1504. This retarder was applied onto the bottom of the timber molds three hours before the casting process, as per the supplier recommendation.

The substrate boxes had a two-phase curing process: Firstly, 15 hours at room temperature curing ($\pm 26^{\circ}\text{C}$) after casting (Figure 16); after this period, the substrates were demolded and the aggregates were exposed with high pressure water jet (Figure 17) which created the roughness required for the repair adhesion.



Figure 16 – Curing process of the concrete substrates before demolding



Figure 17 – Water blasting process

After the blasting process, all the substrates presented similar surface roughness, as presented in Figure 18. Then, the second phase of the curing process took place inside a water tank for 27 days (Figure 19).



Figure 18 – Prepared surface of the concrete substrates



Figure 19 – Water tank for curing process of the concrete substrates

3.2.2.2. Substrate for the four-point bending test

The concrete class and the mixture process was the same as described in section 3.2.2.1. The concrete substrates were cast in metallic forms with dimensions of 50 x 15 x 7.5 cm (W x L x H). The substrate had a two-phase curing process: firstly, 24 hours of room temperature curing ($\pm 26^{\circ}\text{C}$) after casting and subsequent curing inside a water tank for another 27 days.

After the curing process, the substrates were subjected to surface treatment prior to the mortar casting in order to obtain the surface required for the crack trapping mechanism (LIM & LI, 1997); a Black & Decker Circular Saw CS2001 was used to cut and even up the surfaces (Figure 20).

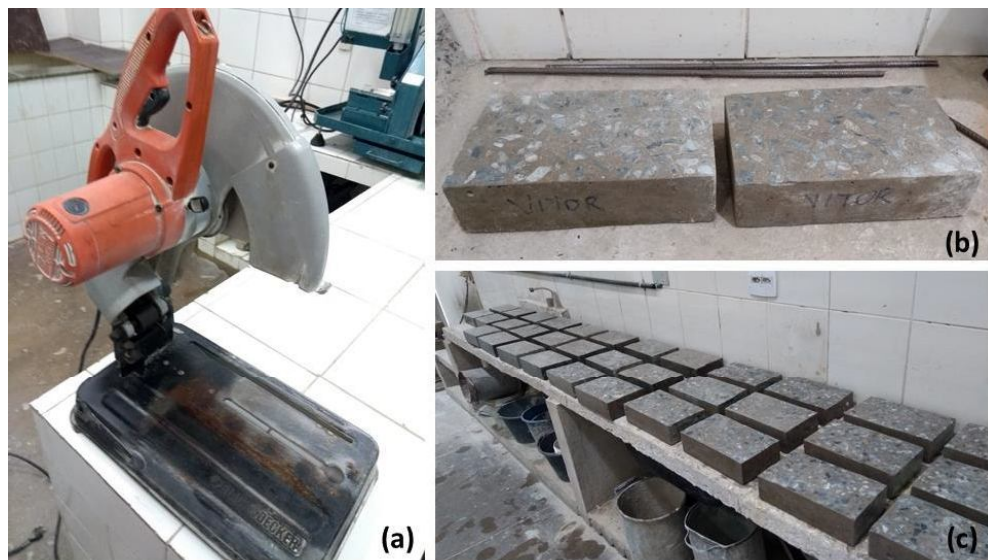


Figure 20 – (a) Circular saw; (b) and (c) samples after surface preparation

To obtain the configuration showed in Figure 10 (section 2.4.2), a smooth tape was used to create regions with no roughness between the two half of substrates and to create the initial notch for the bending test (Figure 21).



Figure 21 – Final preparation of the beams substrates

3.2.3. Alkali-activated repair formulations

During an initial phase, twenty one different formulations were prepared and their mechanical properties assessed (compressive strength and modulus of elasticity). The composition of the matrices varied according to two important factors: (i) the substitution percentage of MK with BFS and (ii) the matrix $[\text{SiO}_2] / [\text{Al}_2\text{O}_3]$ molar ratio. The BFS percentages used were 0%, 20%, 40%, 60% and 80% and the molar ratio $[\text{SiO}_2] / [\text{Al}_2\text{O}_3]$ varied differently within each percentage of MK replacement (Table 3). It is important to note that each group on Table 3 started with a formulation containing no sodium silicate in the activator (G1, G5, G9, G14 and G18). The $[\text{Na}_2\text{O}] / [\text{SiO}_2]$ molar ratio was kept constant to 0.25. The aggregate / binder ratio was also fixed to 1.5 for all formulations.

As an important premise of the entire project, the consistency of all mortars was kept within standard range (255 ± 10 mm) measured according to the flow table method described in the NBR 13276 standard (ABNT, 2016). Both the water content in the mixes and the solution / binder ratio have changed for each formulation to maintain the consistency, as show in Table 3.

Table 3 – Studied formulations

Code	Formulation code	MK (%)	BFS (%)	$[\text{SiO}_2] / [\text{Al}_2\text{O}_3]$	$[\text{H}_2\text{O}] / [\text{Na}_2\text{O}]$	Solution / binder (wt.)
G1	2.0 100MK-0BFS	100	0	2.0	24.1	0.900
G2	2.5 100MK-0BFS			2.5	15.5	0.833
G3	2.75 100MK-0BFS			2.75	13.0	0.903
G4	3.0 100MK-0BFS			3.0	12.0	0.975
G5	2.5 80MK-20BFS	80	20	2.5	18.0	0.815
G6	3.0 80MK-20BFS			3.0	12.5	0.828
G7	3.4 80MK-20BFS			3.4	11.0	0.922
G8	3.8 80MK-20BFS			3.8	10.6	1.059
G9	2.5 60MK-40BFS	60	40	2.5	21.0	0.735
G10	3.0 60MK-40BFS			3.0	14.0	0.710
G11	3.4 60MK-40BFS			3.4	11.0	0.736
G12	3.6 60MK-40BFS			3.6	11.0	0.802
G13	3.8 60MK-40BFS	40	60	3.8	10.5	0.846
G14	3.0 40MK-60BFS			3.0	17.5	0.632
G15	3.4 40MK-60BFS			3.4	12.5	0.600
G16	3.8 40MK-60BFS			3.8	10.5	0.641
G17	4.2 40MK-60BFS	20	80	4.2	10.0	0.728
G18	3.6 20MK-80BFS			3.6	17.0	0.573
G19	3.8 20MK-80BFS			3.8	15.0	0.567
G20	4.2 20MK-80BFS			4.2	11.0	0.535
G21	4.6 20MK-80BFS			4.6	10.0	0.586

3.2.4. Alkali-activated mortars preparation

The twenty-one formulations of the alkali-activated mortars were prepared exactly with the same procedure. Firstly, the raw materials were weighted; the binders (MK and BFS) were manually homogenized before mixing with the solution. The alkali activator solution (sodium silicate, sodium hydroxide and water) were previously mixed and allowed to cool down. The solution was transferred to a mortar mixer and the binders were added in small portions at low speed during 5-10 minutes until the full homogenization of the mix. After this step, the aggregate was added slowly for 2 more minutes. The mixer was then set to high speed for 2 minutes to complete the full homogenization of the mortar.

The flow table test was carried out before casting to ensure the standard consistency of all alkali-activated mortars (Figure 22). As mentioned before, the test procedure followed the NBR 13276 standard (ABNT, 2016).



Figure 22 – Flow table test

Cylinders of (5 x 10) cm (diameter x height) were cast and cured at room temperature ($\pm 26^{\circ}\text{C}$) for mechanical evaluation. The mortars remained in the mold for the first 24 hours and then placed in sealed plastic bags until 28 days when tests were carried out.

The mortar cylinders were subjected to surface treatment prior to mechanical testing in order to allow uniform load distribution; a Metkon SERVOCUT 301 - MM saw was used to even up both ends of the cylinders yet ensuring that the final dimensions were 5 x 10 cm, i.e. height / diameter was equal to 2 (Figure 23).

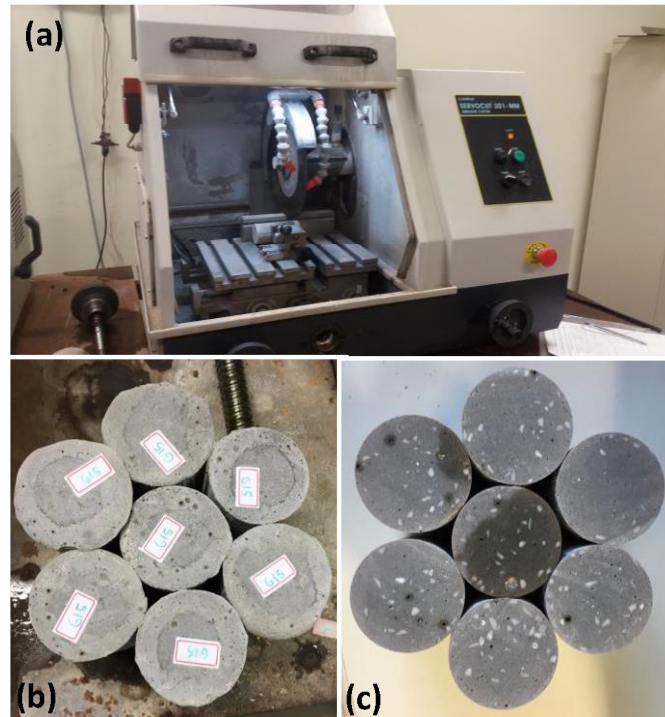


Figure 23 – (a) Metkon saw; (b) samples before and (c) after surface preparation

3.2.5. Substrate-repair panels preparation

Five alkali-activated mortars (out of the initial 21 formulations) were chosen as patch mortars and were applied onto the concrete substrate for adhesion evaluation. Those five formulations were chosen according to their compressive strength and modulus of elasticity (section 4.2.2). Ten panels were cast, 5 with addition of 0.25% vol. PP fiber and another 5 without fiber reinforcement. One panel was cast with the commercial structural mortar as reference.

It is important to note that, at this stage, the PP fibers were used in the mortars only to mitigate the early-age shrinkage and possibly affect the adhesion between the repair mortar and concrete substrate. The results (section 4.3.1) will show the effect of the amount of fiber (0.25% vol.) on pull-off testing.

The preparation process of mortars containing PP fibers was essentially the same as described in section 3.2.4, except for the addition of fibers, which took place at the end of the mixing process. Another 1-minute high-speed mixing after fiber addition ensured proper dispersion of the fibers.

After the mixing process, these mortars were horizontally applied onto the concrete substrates (20 mm thick) with subsequent compaction in a vibrating table (Figure 24).

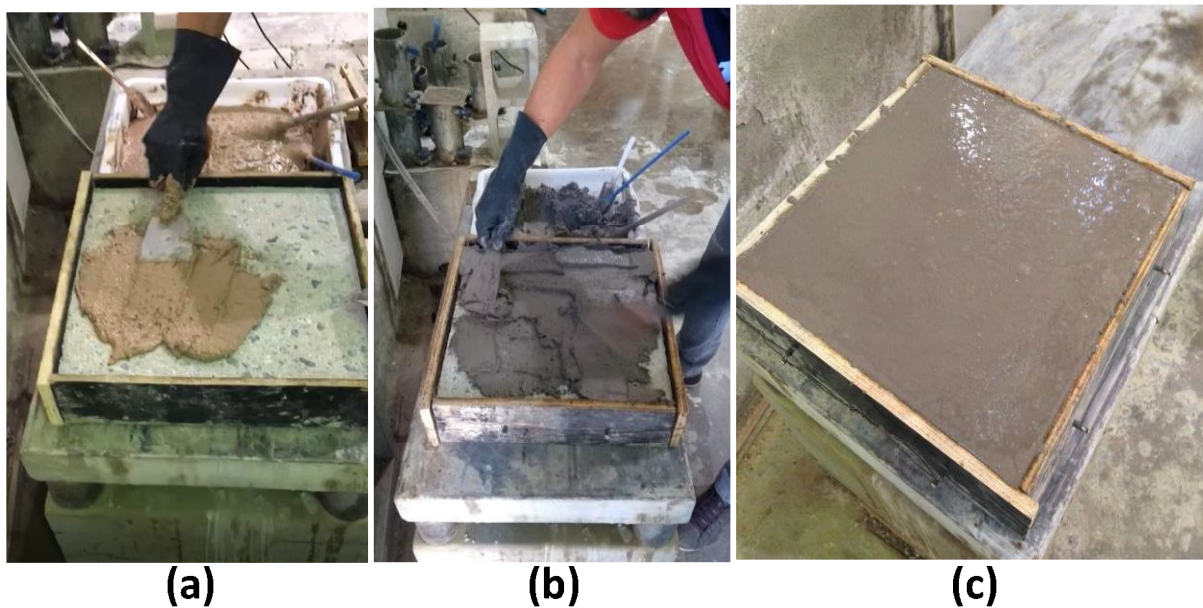


Figure 24 – Alkali-activated mortar: (a) and (b) being applied and (c) after vibrating process

According to the British Standard BS EN 1542 (1999), any formwork must be removed from the panel 24 hours after the mortar placement. The panel shall be then stored for subsequent curing process in a vertical position. The panels were then horizontally cured at room temperature ($\pm 26^{\circ}\text{C}$) during the first 24 hours, demolded and vertically cured for another 27 days prior to pull-off testing.

3.2.6. Substrate-repair beams preparation

According to the results obtained from the pull-off test (section 4.3.1), it was decided to exclude the G18 (3.6 20MK-80BFS) formulation. Therefore, only four formulations (G4, G6, G16 and G17) were tested under flexion (four-point bending test). Sixteen beams were cast, 8 with 0.25% vol. PP fiber and another 8 without fiber reinforcement, four of each formulation. In addition, two other beams were cast with the commercial structural mortar. The results (section 4.3.2) will show the effect of the amount of fiber (0.25% vol.) on the crack trapping mechanism test.

The mortars mixing process was basically the same described for the panels, except for the fact that the bench top mortar mixer was replaced with a manual mixer (Figure 25) due to the higher volume of mortars produced for the beams.



Figure 25 - Mixing process of the repair mortar beams

After the mixing process those mortars were cast over the concrete substrates beams (50 x 15 x 7.5 cm (W x L x H)), with subsequent compaction in a vibrating table (Figure 26).



Figure 26 - (a) Substrate in metallic form; (b) casting of the AAM and (c) compaction process

The beams were cured at room temperature ($\pm 26^{\circ}\text{C}$) during the first 24 hours, then demolded and stored under a black tarpaulin for another 27 days prior to four-point bending testing.

3.2.7. Mechanical evaluation

Cylindrical samples from both the Portland cement concrete formulation (used for the substrate) and alkali-activated mortars were subjected to compressive strength and modulus of elasticity tests. Both tests were carried out using a universal

press Emic D30000 (Figure 27). A 300 kN load cell was used to test 5 x 10 (cm) alkali-activated mortar cylinders at 0.25 ± 0.05 MPa/s loading rate (NBR 7215) (ABNT, 1996). Concrete samples (10 x 20 cm) were tested using a 2000 kN lead cell; the test loading rate was 0.45 ± 0.15 MPa/s as per the standard NBR 5739 (ABNT, 2007).



Figure 27 – Universal press used for mechanical tests

The static modulus of elasticity of both, concrete and mortars, was determined according to NBR 8522 (ABNT, 2008). The loading and unloading rate was 0.45 ± 0.15 MPa/s, following the methodology presented on NBR 8522 (Figure 28). A strain gauge was used to register the deformation during the test (Figure 29).

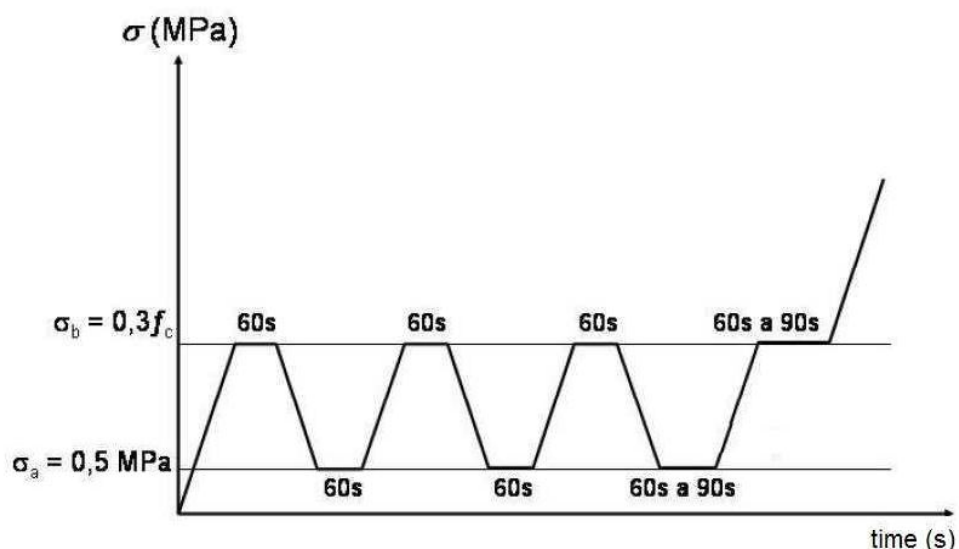


Figure 28 – Loading schematic representation to determine the modulus of elasticity (adapted from (ABNT, 2008))

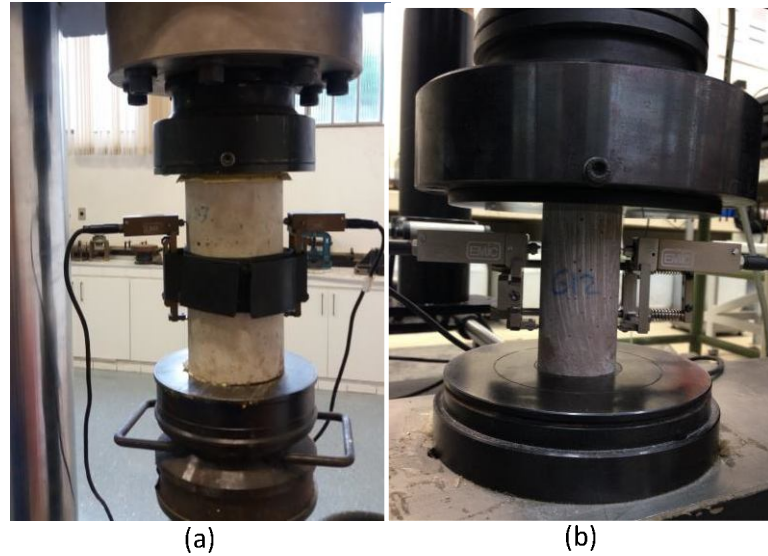


Figure 29 – Modulus of elasticity test for (a) concrete and (b) alkali-activated mortars

3.2.8. Substrate-repair adhesion evaluation

The substrate-repair adhesion evaluation proposed in this study is composed of two different characterizations tests. The first step is the evaluation of the bond strength using direct tension test (pull-off testing). This test results are presented in section 4.3.1. The second step is the evaluation of the crack and delamination behavior using the four-point bending (crack trapping mechanism). This test results are presented in section 4.3.2

Visual analysis and high quality pictures were used to assess the failure mechanisms for all tests, in order to ensure a complete interface characterization between the repair mortar and the concrete substrate.

3.2.8.1. Bond strength by pull-off test

The bond strength test was carried out according to the method described in section 2.4.1. Eight pull-off tests were performed for each substrate-repair panel; the preparation started after the curing period of the panels (28 days), by drilling 40 mm holes (20 mm of the repair mortar and another 20 mm into the substrate) using a Schulz Pratika FSB 16P bench-drilling machine with a 50 mm diamond circular saw. A wet-drilling process was used to avoid the saw deterioration and as indicated by the supplier (Figure 30).



Figure 30 – Drilling process

Twenty-four hours after the drilling process - time needed for the panel to dry out - the circular dollies were glued over the drill spots with the epoxy resin bonding agent Sikadur 32. The bonding agent was previously prepared as the supplier instructions by mixing its two components in a 2:1 weight ratio. Any impurities were removed from the mortar surface in order to ensure proper bond between the dolly and the mortar surface; the epoxy resin was applied onto both surfaces (dolly and mortar) in thin layers (Figure 31).



Figure 31 – Setting the dollies distribution on the substrate-repair panel

The epoxy resin was allowed 24 hours to set; then, pull-off tests were carried out using a Haftprufer Pull-off Tester DYNA proceq Z16. The load was manually applied in a rate of 0.05 MPa/s. Every specimen was visually assessed to determine the type of failure according to BS EN 1542 (1999) (Figure 32). The percentage of

each failure region (substrate, repair or interface) was obtained from an average value of the eight specimens of each panel.

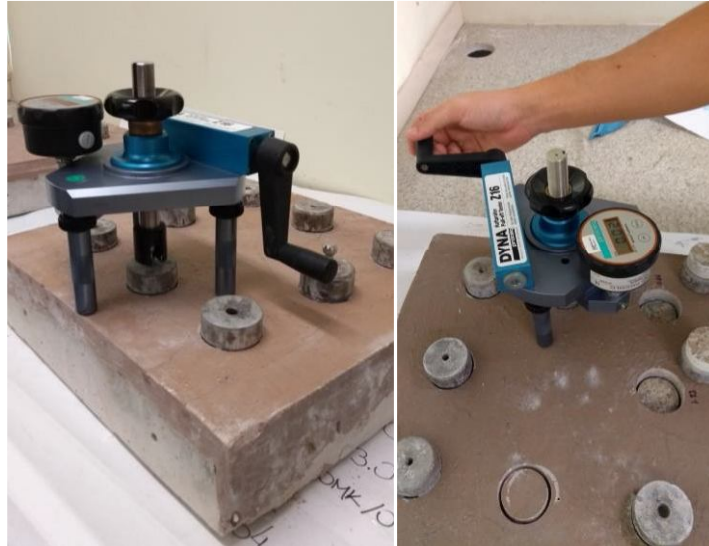


Figure 32 – Pull-off test

3.2.8.2. Crack Trapping Mechanism by four point bending

The crack trapping mechanism developed by Lim and Li (1997) described on section 2.4.2 was used to evaluate the crack and delamination behavior of the repair mortars. This evaluation was carried out for the formulations cited in section 3.2.6 using the same universal press (Emic D30000, Figure 27). A 300 kN load cell was used; the deflection rate was 0.005 mm/s. A strain gauge was used to register the deflection during the test (Figure 33). An interface analysis was carried out after the failure to determine the crack propagation pattern.



Figure 33 – Four point bending test

3.2.9. Physical evaluation

The physical properties of the repair mortars were also addressed in this study. The tests used to estimate the durability of the alkali-activated repair mortar were water absorption, apparent density and apparent porosity.

Water absorption, apparent density and apparent porosity was determined by using the water saturation method presented on NBR 9778 (ABNT, 2005). The samples were oven dried for 24 hours; after that the dry weight (m_1) was registered. The samples were then placed inside a water tank for 120 hours to allow full saturation, after which the saturated weight under water (m_2) and the saturated surface dry weight (m_3) were measured.

4. RESULTS

4.1. CHARACTERIZATION OF RAW MATERIALS

The chemical composition provided by the suppliers of the raw materials (MK, BFS and sodium silicate) is shown in Table 4.

Table 4 – Raw materials chemical composition

Materials	SiO ₂	Al ₂ O ₃	Na ₂ O	K ₂ O	CaO	H ₂ O	MgO	Fe ₂ O ₃
MK (%)	43.55	37.00	-	-	0.05	-	0.05	2.00
BFS (%)	34.95	12.63	-	0.93	39.87	-	5.38	2.30
Na ₂ SiO ₃ (%)	31.79	-	15.00	-	-	53.21	-	-

Figure 34 presents the XRD pattern for both precursors, MK and BFS. It is possible to see that both materials are essentially amorphous (91% for the MK and 98% for the BFS – calculated from XRD pattern), ensuring the high reactivity needed for the alkaline activation.

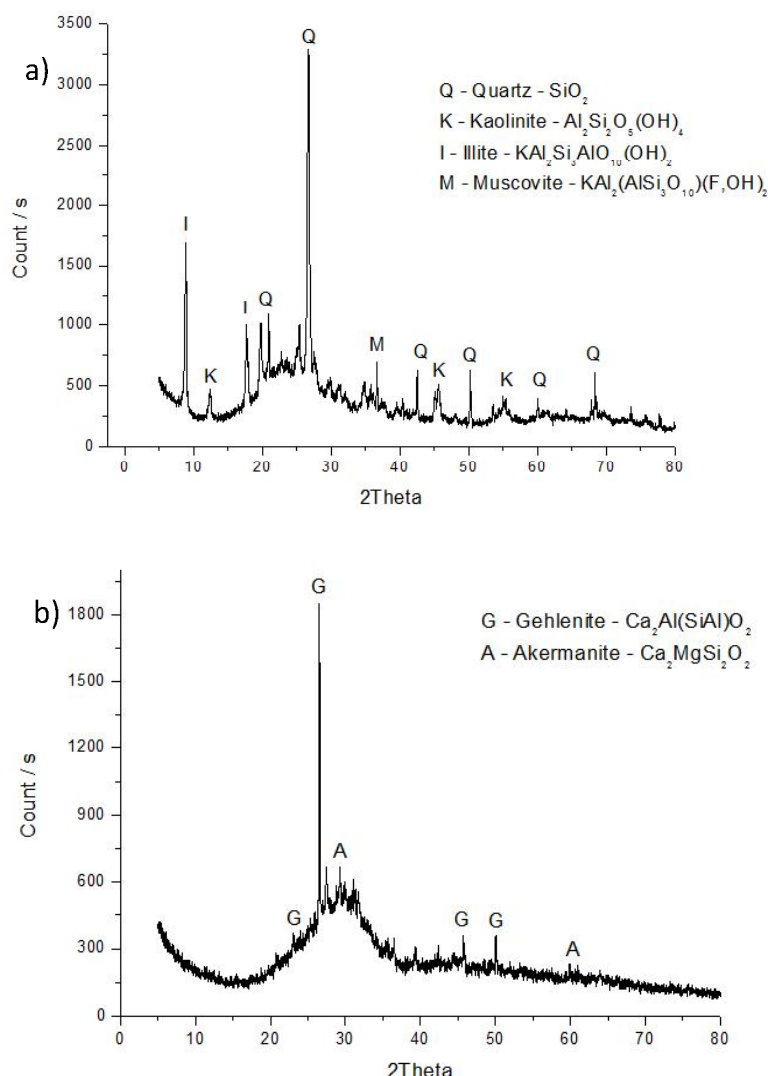


Figure 34 – Diffractometer: (a) MK and (b) BFS

The particle size distribution of both precursors is shown in Figure 35; the average particle size of MK is 2.12 μm and of BFS is 8.75 μm . This figure shows that the MK particles are considerably thinner than the BFS ones, the latter demanding less solution – or lower $[\text{H}_2\text{O}] / [\text{Na}_2\text{O}]$ molar ratio - for the same consistency (Table 3, section 3.2.3). Pycnometry tests determined that the apparent density for MK and BFS were, respectively, 2.59 g/cm^3 and 2.86 g/cm^3 .

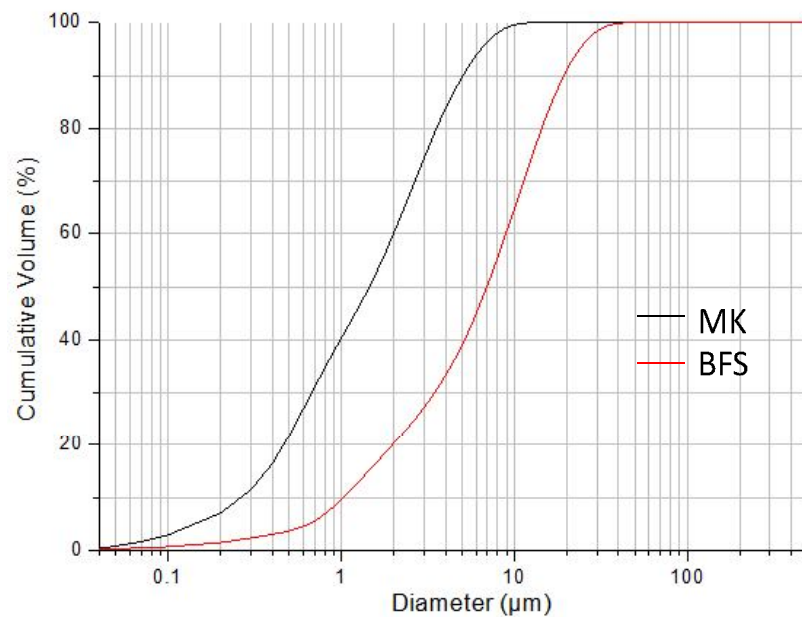


Figure 35 – Particle size distribution of MK and BFS

The dolomite used as fine aggregate to produce the repair mortars has a fineness modulus of 2.49 and its particle size distribution (PSD) is shown in Figure 36, along with the thick and thin (optimum) envelopes (dashed lines) for concrete fine aggregate according to the Brazilian standards. It is important to note that the aggregate PSD lies in the optimum envelope (dashed brown lines), so it is suitable for concrete production. The aggregate properties were obtained according to NBR NM 248 (ABNT, 2003).

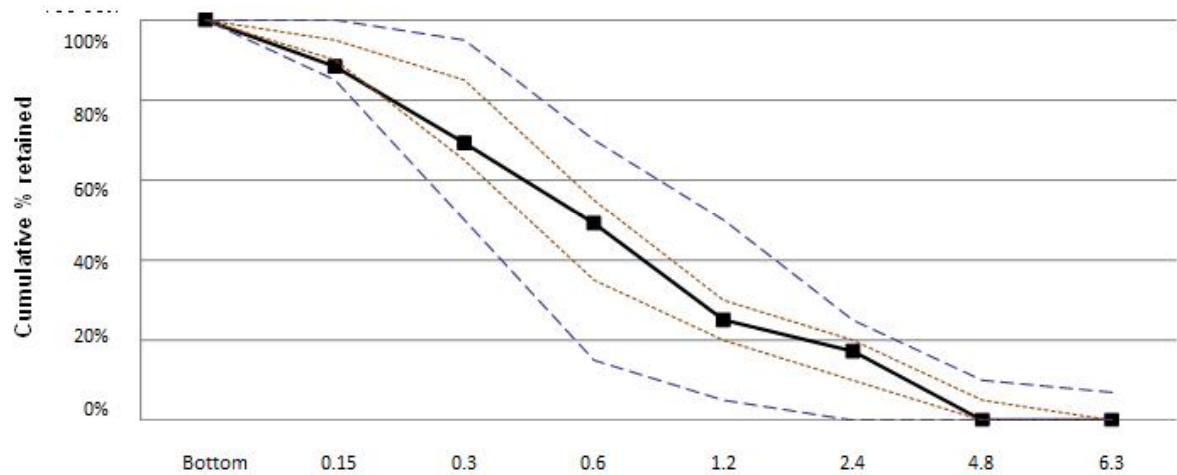


Figure 36 – Dolomite aggregate particle size distribution

4.2. COMPATIBILITY

4.2.1. Fresh Properties

The workability of the fresh alkali-activated mortars is presented in Table 5. All twenty-one formulations had their consistency between the fixed range (255 ± 10 mm).

Table 5 – Consistency of fresh mortars

Formulations	Flow table test (mm)
2.0 100MK-0BFS	243
2.5 100MK-0BFS	245
2.75 100MK-0BFS	250
3.0 100MK-0BFS	245
2.5 80MK-20BFS	242
3.0 80MK-20BFS	267
3.4 80MK-20BFS	258
3.8 80MK-20BFS	245
2.5 60MK-40BFS	265
3.0 60MK-40BFS	263
3.4 60MK-40BFS	247
3.6 60MK-40BFS	247
3.8 60MK-40BFS	245
3.0 40MK-60BFS	248
3.4 40MK-60BFS	243
3.8 40MK-60BFS	264
4.2 40MK-60BFS	248
3.6 20MK-80BFS	255
3.8 20MK-80BFS	245
4.2 20MK-80BFS	260
4.6 20MK-80BFS	257

4.2.2. Mechanical Properties

The mechanical properties of the concrete used as substrate were 32.75 ± 0.96 MPa for compressive strength and 26.80 ± 0.59 GPa for modulus of elasticity at 28 days. These results agree with the mix design (concrete Class C30) for the substrate.

Figure 37 presents the compressive strength results of the alkali-activated mortars against the $[\text{SiO}_2] / [\text{Al}_2\text{O}_3]$ molar ratio. Overall it is possible to see that the compressive strength increased for higher $[\text{SiO}_2] / [\text{Al}_2\text{O}_3]$ molar ratio. The majority of the formulations have their compressive strength between 40-60 MPa. Some have their values under 15 MPa, mostly because of the low $[\text{SiO}_2] / [\text{Al}_2\text{O}_3]$ value and the absence of sodium silicate in the activator. Few (only two at the top right) have values above 80 MPa due to the high content of BFS and silicate combined in their compositions.

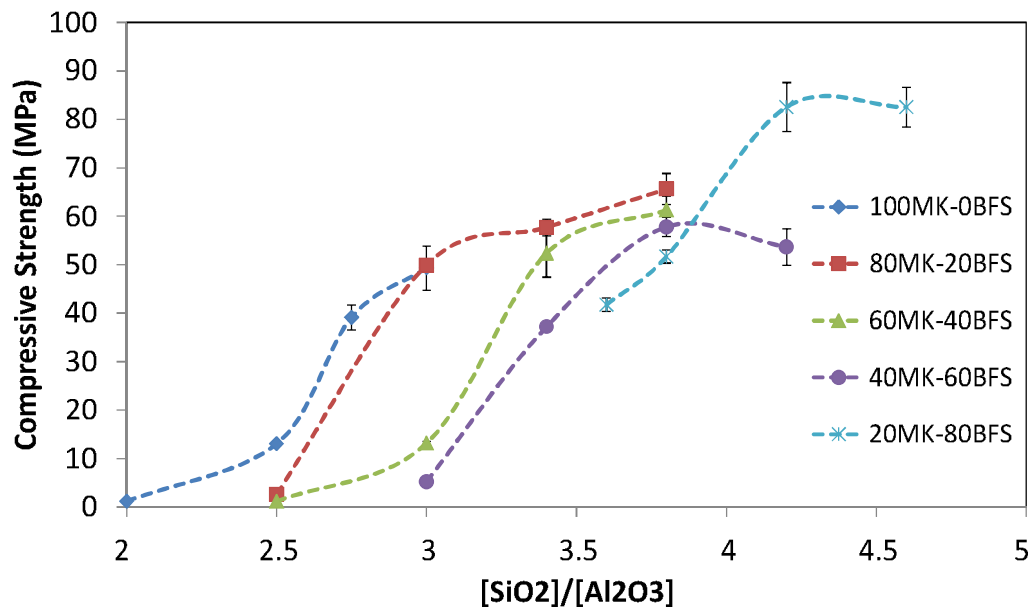


Figure 37 – Compressive strength versus $[\text{SiO}_2] / [\text{Al}_2\text{O}_3]$ molar ratio for alkali-activated mortars

Basically the same rise in strength was observed in all five groups of MK-BFS mortars. In addition, it is important to highlight that the neat MK mortars (100MK-0BFS) could not be produced with $[\text{SiO}_2] / [\text{Al}_2\text{O}_3]$ molar ratios higher than 3.0; in fact, higher $[\text{SiO}_2] / [\text{Al}_2\text{O}_3]$ ratios would demand larger volumes of sodium silicate that increase the stickiness of the mixes and jeopardize the mixing and casting. The employment of BFS, however, allows the design of formulations with higher $[\text{SiO}_2] / [\text{Al}_2\text{O}_3]$ ratios without the need for increasing the silicate content.

Figure 38 presents the modulus of elasticity results against the same activation parameter ($[\text{SiO}_2] / [\text{Al}_2\text{O}_3]$ molar ratio). The majority of the formulations have their

modulus of elasticity between 15-18 GPa, which is in line with the results of the literature for these type of alkali-activated matrices (NĚMEČEK *et al.*, 2011; PROVIS & VAN DEVENTER, 2014; PACHECO-TORGAL *et al.*, 2015). Some formulations have their modulus of elasticity values under 10 GPa, in agreement with their low compressive strength. The two at the top right present values above 25 GPa due to the high content of BFS and silicate combined in their compositions, also in line with the highest compressive strength.

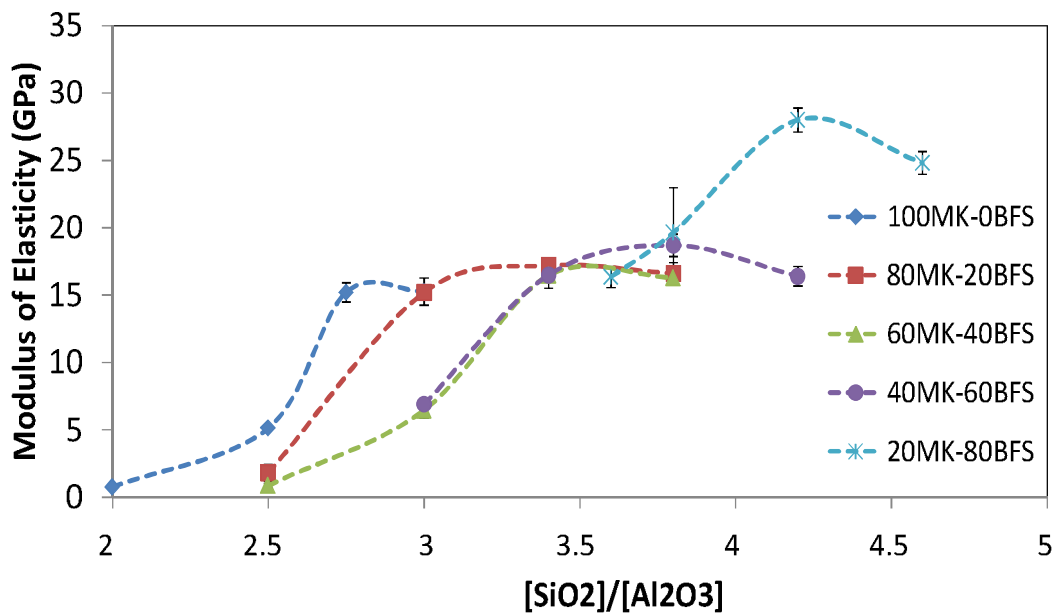


Figure 38 – Modulus of elasticity versus $[\text{SiO}_2] / [\text{Al}_2\text{O}_3]$ molar ratio

As presented in section 2.3, the structural compatibility between the substrate and the repair material depend on some requirements, including the mechanical strength and the modulus of elasticity. According to Emmons *et al.* (1993) the repair material needs to have a higher compressive strength and equivalent modulus of elasticity to the substrate. As shown in Figure 38 a single formulation (4.2 20MK-80BFS) achieved a modulus of elasticity as high as that of the concrete substrate. However, such higher BFS and silicate content in this mix increased the susceptibility to shrinkage and cracking.

Therefore, it was decided to choose five formulations (out of the twenty-one) for further studies; they comply with the compressive strength requirement (>33 MPa) and present approximately the same modulus of elasticity (15-17 GPa), the latter far below the 27 GPa of the concrete. Any delamination issues due to the incompatibility between the modulus of elasticity will be assessed on the proposed adhesion evaluations, i.e. Pull-off test and crack trapping test.

Each of the five formulations chosen contains a different ratio between MK and BFS, i.e. 0%, 80/20, 60/40, 40/60 and 20/80 (Table 6); The formulation G18 (3.6 20MK-80BFS) presented slightly lower compressive strength than the others, which is due to the absence of sodium silicate in the activator.

Table 6 – Chosen formulations properties

Code	New code	Formulation	Solution / binder	Flow table (mm)	Compressive Strength (MPa)	Modulus of elasticity (GPa)
G4	3.0-100/0	3.0 100MK-0BFS	0.975	245	49.32	15.27
G6	3.0-80/20	3.0 80MK-20BFS	0.828	267	49.94	15.20
G12	3.6-60/40	3.6 60MK-40BFS	0.802	247	56.36	16.80
G17	4.2-40/60	4.2 40MK-60BFS	0.728	248	53.65	16.40
G18	3.6-20/80	3.6 20MK-80BFS	0.573	255	41.74	16.35

4.3. ADHESION PROPERTIES

4.3.1. Pull-Off test

As described in section 3.2.8.1 eleven panels were used to assess adhesion bond by pull-off testing. The bond strength results from the pull-off test are present in Table 7 and in Figure 39. This table presents the maximum and the average bond strength as well as the region of failure and it's combinations for each panel, according to the BS EN 1542 recommendation (EN, 1999). The suffix (FR) after the panel code accounts for 0.25% PP fiber reinforcement. The commercial PC repair mortar (Ref.) was used for comparison.

Figure 39 shows the average bond strength values as a function of the BFS content and the percentage of failure on the substrate region. None of the repair mortar meets the class R4 (structural) requirement of the standard EN 1504-3 (EN, B., 2005). 3.0-100/0, 3.0-100/0FR, 3.0-80/20, 3.0-80/20FR and 4.2-40/60FR presented values above the limit required by the standard EN 1504-3 (EN, B., 2005) for classes R1 and R2 (non-structural) and for class R3 (structural). 3.6-60/40, 3.6-60/40FR and 4.2-40/60 meet the requirement only for non-structural repairs (classes R1 and R2). 3.6-20/80, 3.6-20/80FR and the commercial mortar do not meet any requirement of any class of repair mortars present by EN 1504-3 (EN, B., 2005) (Table 2).

Table 7 – Bond strength results

Code	Panel	Maximum bond strength (MPa)	Average bond strength (MPa)	Region of failure	Combination of failure regions
3.0-100/0	3.0 100MK-0BFS	2.17	1.78	A : A/B	75% : 25%
	3.0 100MK-0BFS (FR)	2.13	1.63	A : A/B : B	70% : 25% : 5%
3.0-80/20	3.0 80MK-20BFS	2.12	1.74	A : A/B	70% : 30%
	3.0 80MK-20BFS (FR)	2.27	1.74	A : A/B	65% : 35%
3.6-60/40	3.6 60MK-40BFS	1.27	1.09	A : A/B	70% : 30%
	3.6 60MK-40BFS (FR)	1.42	1.33	A : A/B	75% : 25%
4.2-40/60	4.2 40MK-60BFS	1.38	0.99	A : A/B : B	55% : 35% : 10%
	4.2 40MK-60BFS (FR)	1.99	1.65	A : A/B	45% : 55%
3.6-20/80	3.6 20MK-80BFS	0.57	0.29	A/B	100%
	3.6 20MK-80BFS (FR)	0.77	0.52	B	100%
Ref.	Commercial mortar	0.35	0.24	A/B : B	65% : 35%

(FR: fiber-reinforced, A: failure in the substrate, B: failure in the repair mortar, A/B: failure in the interface between repair and substrate)

These results show a considerable standard deviation, which is quite common in pull-off tests. In general, it is possible to say that, the higher the % of BFS the lower is the bond strength, which may be related to the lower soluble silica content (or sodium silicate) in those formulations (KHAN *et al.*, 2014), since the amount of silicate is lower for high contents of BFS. In that sense, sodium silicate either (i) promotes the alkali-activation and consequently the bond between repair and substrate or (ii) act as a bond agent *per se*.

Is also possible to conclude that the presence of fiber slightly helped the adhesion of the repair mortar increasing the average bond strength in most of the cases (ZANOTTI *et al.*, 2017). However, the PP fiber has a remarkable effect when the bond strength is reduced, which is the case for 3.6-60/40, 4.2-40/60 and 3.6-80/20.

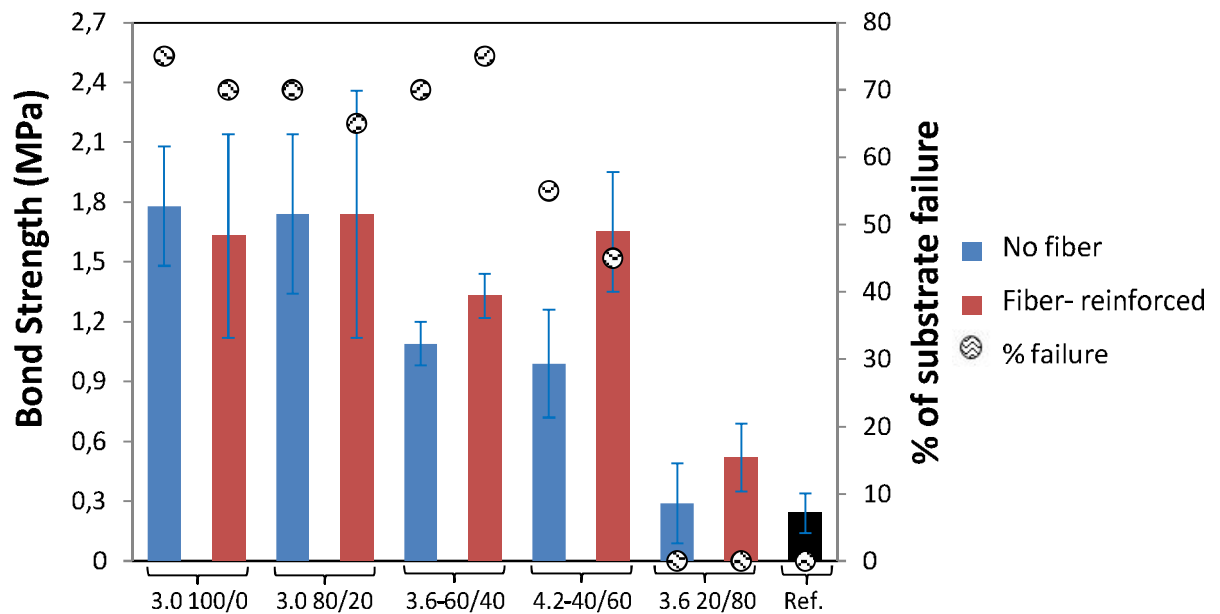


Figure 39 – Bond strength results obtained by pull-off test

A visual assessment was also carried out to determine the type of failure presented in Table 7. Overall, the failure pattern of the panels was quite similar, i.e. either on the interface or in the concrete substrate. This behavior shows a good adhesion between the repair mortar and the substrate, due to chemical reaction between cations from the substrate surface and the ions from the alkali activated binders (PACHECO-TORGAL *et al.*, 2008A). The panels 3.6-20/80, however, presented poor performance, with 100% failure in the interface (unreinforced) and 100% in the repair mortar when PP fiber reinforced. This is somehow expected, as the mortars do not contain sodium silicate in the composition; their poor performance is in line with their lower compressive strength. Some samples after the pull-off test are presented in Figure 40 to illustrate the types of failure obtained.

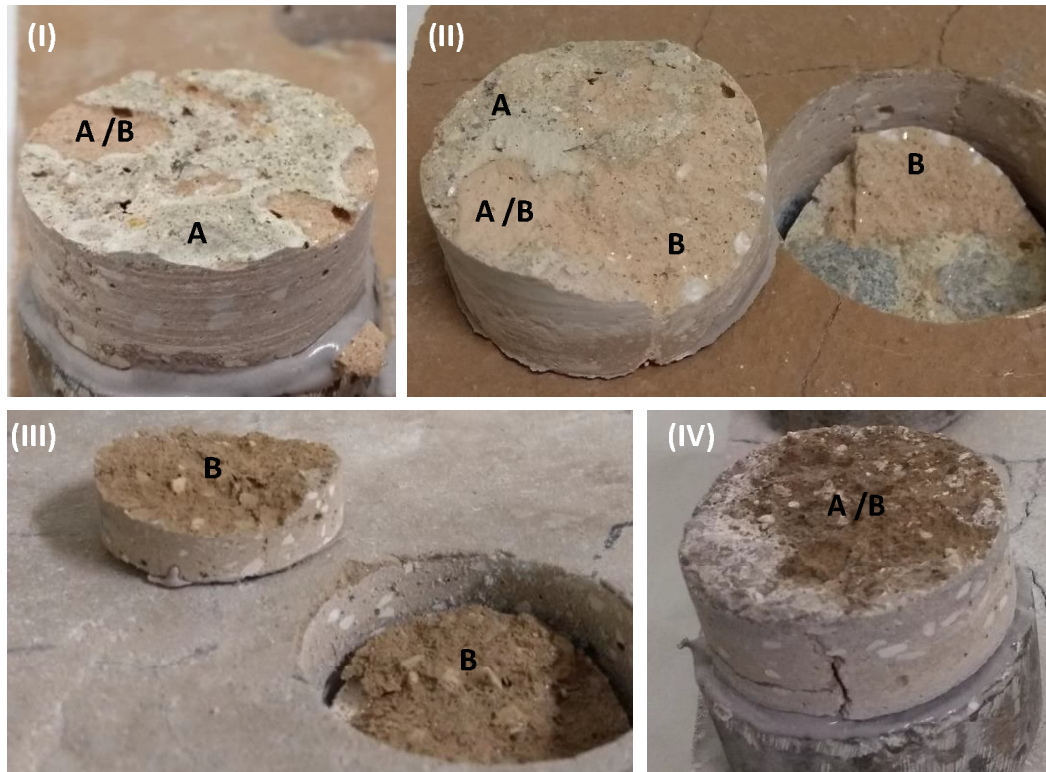


Figure 40 - Failure samples after pull-off test: (I) A : A/B, (II) A : A/B : B, (III) B and (IV) A/B

Regarding the adhesion properties, 3.0-80/20FR appears to be the most promising formulation for repair applications; firstly, it meets the EN 1504-3 (EN, B., 2005) requirements for R1, R2 and R3 classes (Table 2, section 2.4.1). It also has the highest maximum bond strength and a high percentage of failure in the substrate, showing a good adhesion to the concrete. On the other hand, the 3.6-20/80, 3.6-20/80FR and the commercial mortar are not suitable for repair applications.

4.3.2. Crack Trapping Mechanism Test

As described in section 3.2.8.2 eighteen beams were used to evaluate the crack and delamination behaviors via four-point bending test. The load-displacement behaviors for all cases are illustrated in Figure 41. It is possible to notice the high stiffness of all repair mortars, which is typical of brittle materials. A significant increase in deflection after failure can be observed in all cases of fiber-reinforced mortars, compared with its analogue without fibers. The fiber incorporation significantly affected the energy absorption capacity, but not necessarily the ultimate load. Figure 42 illustrates how the fibers work bridging the cracks after the matrix failure.

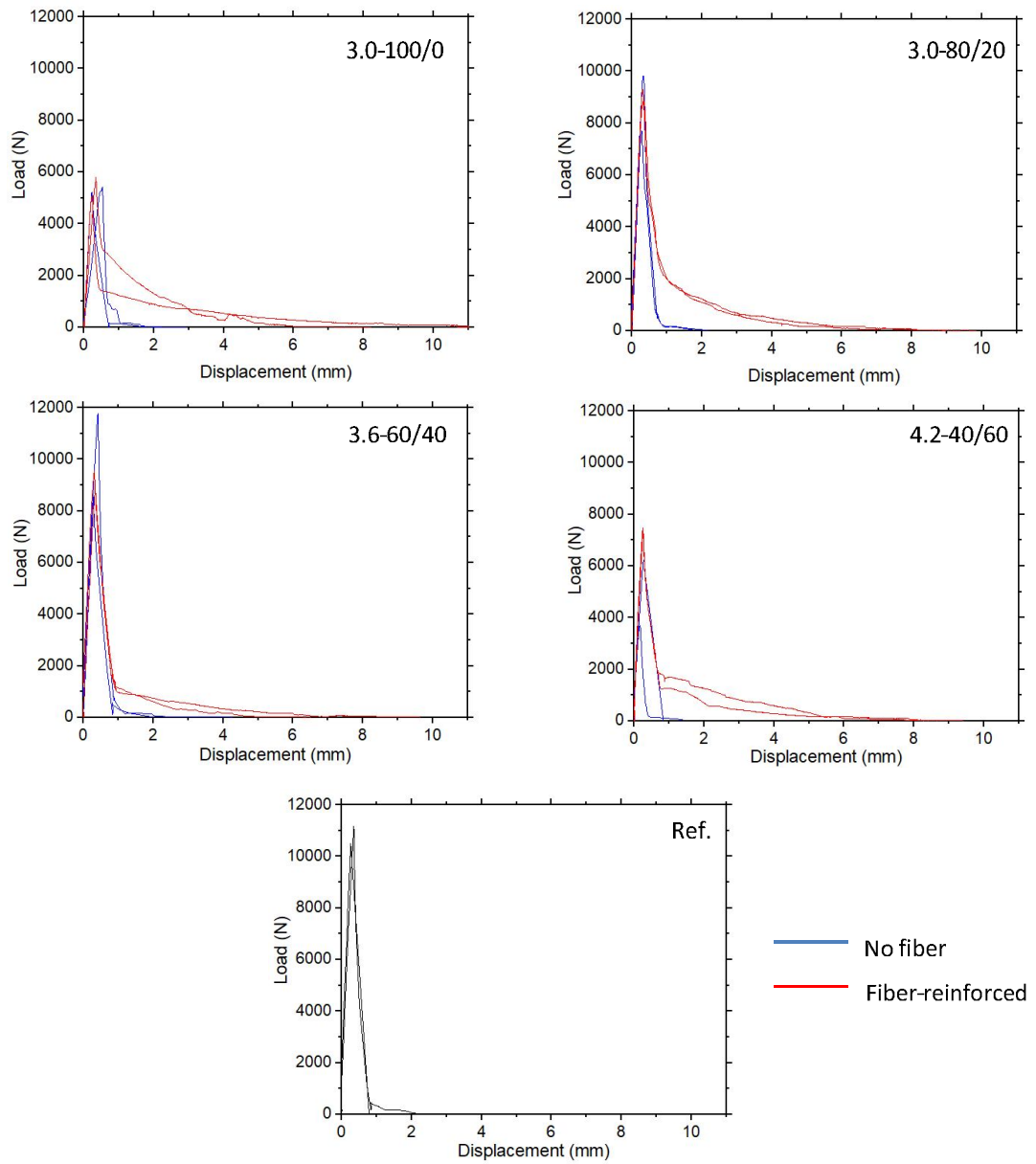


Figure 41 – Load x displacement curves

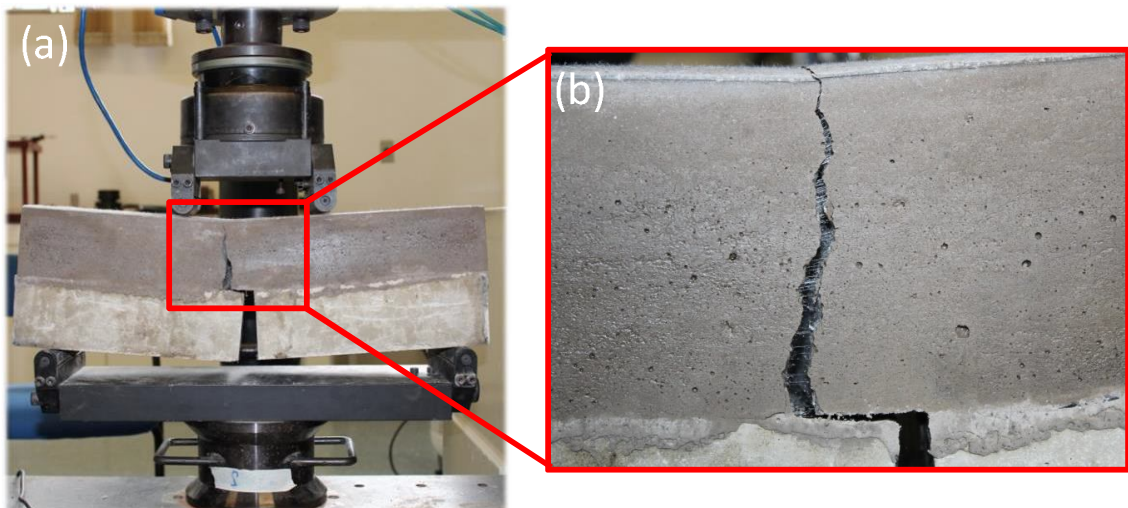


Figure 42 – (a) flexural tensile test and (b) detail of a fiber-reinforced cracking beam

Figure 43 shows the flexural strength values of all eighteen beams; each bar in this figure combines the results of the two individual beams tested (hatched and solid bars). Overall the flexural strength varied between 2.0 to 6.5 MPa. The beams cast with repair mortars without fiber reinforcement (blue bars) presented larger strength variations, compared to those with PP fibers (red bars). That might be explained by the fact that AAM matrices (as any other brittle materials) are very stiff and may present a sudden failure due to any internal defect (i.e. micro cracks); the fibers somehow mitigate this effect by bridging the cracks. However, the presence of fiber in the repair mortar didn't show a positive influence on the flexural strength, as PP fibers are characterized by a low strength and modulus of elasticity; therefore it is not surprising that in some cases the flexural strength decreased with PP fiber addition. BFS appears to help increase the flexural strength up to 40% replacement (for both cases, no fiber and fiber-reinforced); the reduction at 60% replacement is likely to be related to the low silicate content in that repair mortar, rather than the amount of BFS per se.

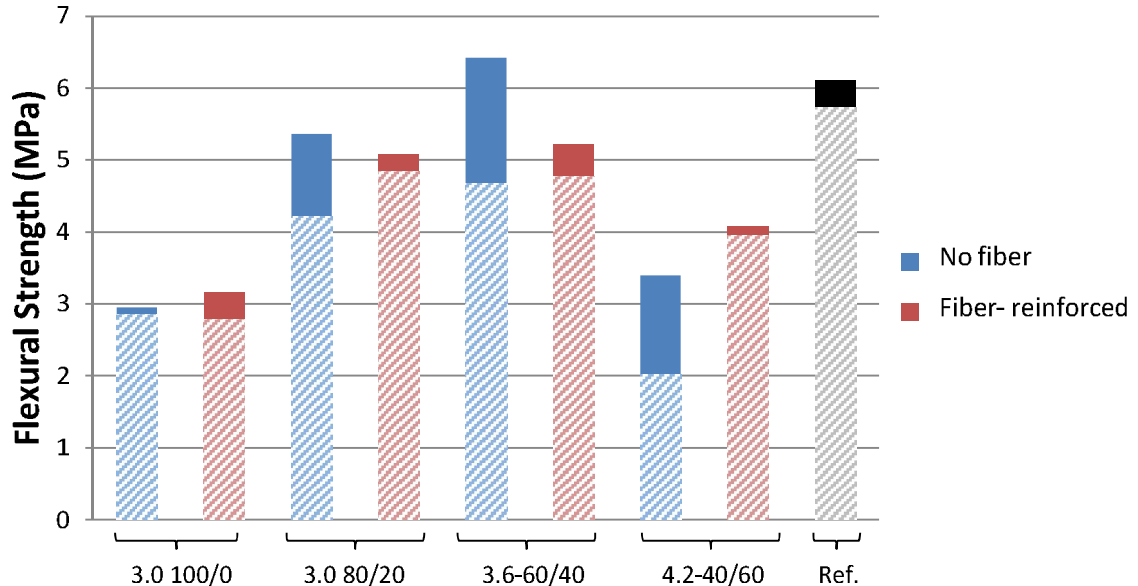


Figure 43 – Flexural strength of both beams of each formulation

Figure 44 shows the crack and delamination patterns as main evaluation parameters of the crack trapping mechanism test. The delamination process occurred only on two samples of the 3.0-100/0 as shown in Figure 44 and highlighted in Figure 45. Figure 45a presents the main cause for the delamination problem; the beams that suffered this process were already cracked on the interface between

substrate and mortar before the bending test, probably due to excessive drying shrinkage. In fact, 3.0-100/0 is the formulation with the highest solution / binder ratio (Table 6, section 4.2.2) and it is known that an excess of water in AAM MK-based leads to shrinkage problems (PROVIS, BÍLEK, *et al.*, 2014). Figure 45b shows the delamination in process during the bending test. Zanotti *et al* (2017) have already observed shrinkage in 100% MK alkali-activated repair mortars cured at room temperature. The results presented here confirm that small additions of BFS will somehow help prevent this issue, as (i) the strength development and stiffness is increased at room temperature; (ii) the lower water demand reduced the susceptibility to drying shrinkage.

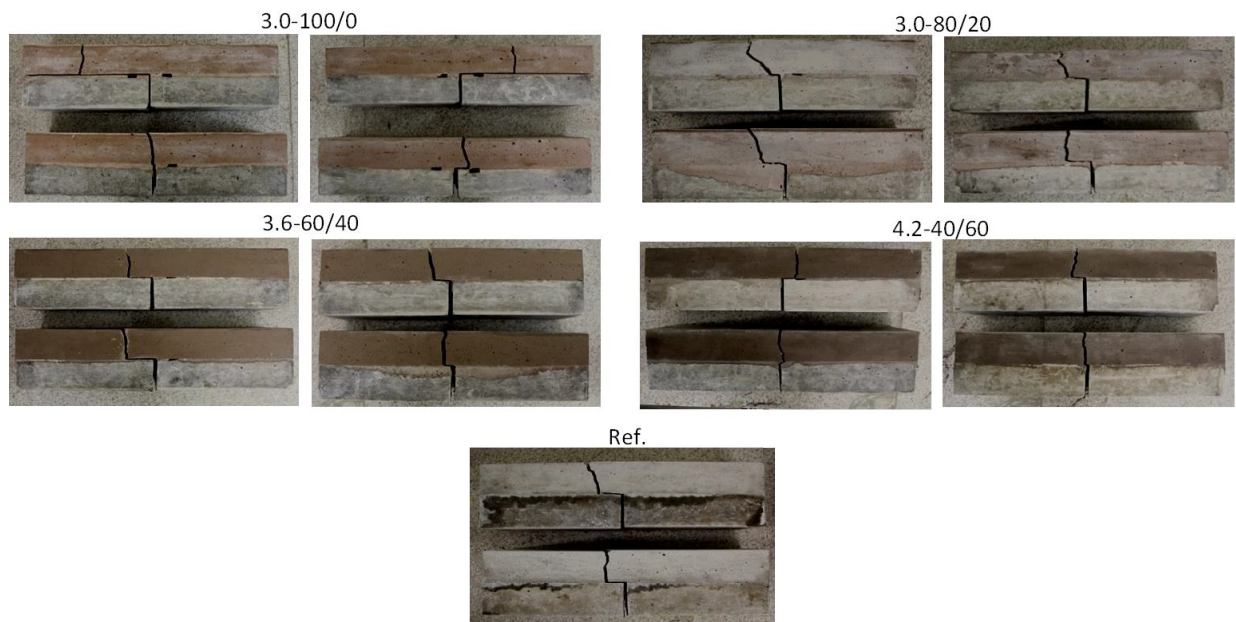


Figure 44 – Cracking pattern after bending test (for each formulation: left side - no fiber; right side - fiber reinforced)

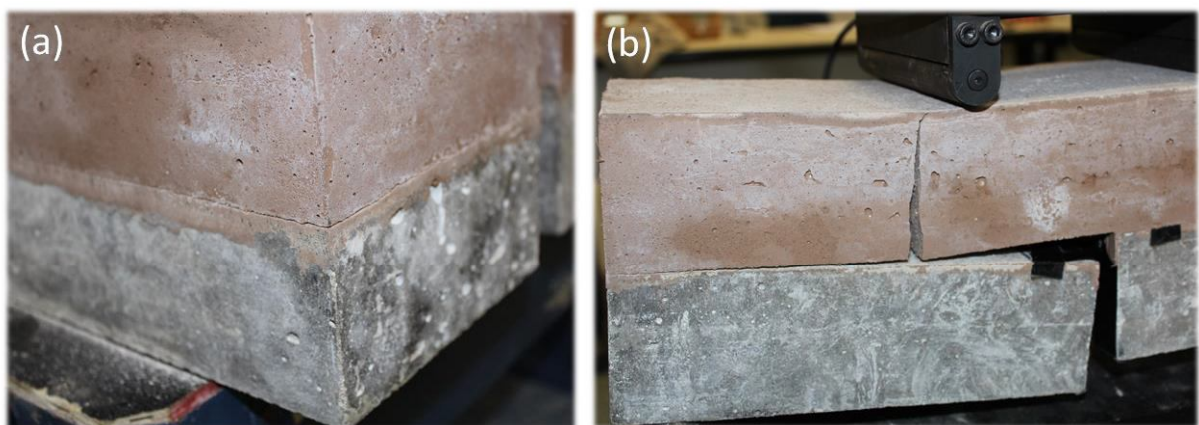


Figure 45 – Delamination problem: (a) fissured interface before test and (b) failure beam with high delamination on the interface

Both beams with mortars 3.0-80/20 and 3.6-60/40 presented a crack development very similar to the reference mortar (PC based), which is typical for brittle materials: first the crack propagates along the interface on the initial notch (smooth tape region) and then kinked out to the repair material right at the end of the tape, with a consequent sudden load drop. This behavior shows that the bond strength at the interface is stronger than the repair mortar.

The beams with the mortar 4.2-40/60 behave differently: the crack propagation in the repair mortar started much earlier, while in the smooth tape region. This indicates that the material must have more defects and consequently lower resistance to crack propagation, which is by the way in line with the low flexural strength of that particular mortar.

Finally, it is important to note that in all cases the fractured halves of the specimens separated completely. So, the concept of the trapping behavior proposed to repair materials by Lim and Li (1997) and showed in Figure 11 (section 2.4.2) couldn't be found in any of the tested formulations. In fact, the test was originally developed for strain-hardening materials, which is not the case herein.

As for the Pull-off test, the 3.0-80/20FR appears to be the most promising formulation for repair applications; showing the best deformation capacity among the others, an ultimate flexural strength similar to the commercial mortar and an interesting crack development pattern without delamination problem.

4.4. PHYSICAL PROPERTIES

As described in section 3.2.9 the physical properties (water absorption, apparent porosity and apparent density) were assessed to evaluate the indicative of durability of the repair mortars.

Figure 46 presents the results of water absorption and of porosity. The water absorption values varied between 9.0% and 15.5% and the porosity values between 20.0% and 27.5%. Those results are very consistent, given that the material water absorption is directly related to its porosity.

It can be noticed that the higher the percentage of BFS employed, the lower is the water absorption and apparent porosity, which is a result from the densification of the blended alkali-activated matrix. This behavior was expected according to the literature (BERNAL *et al.*, 2011; BERNAL *et al.*, 2013; BORGES *et al.*, 2016; SAMSON *et*

al., 2017). The presence of fiber slightly decreased both properties in all formulations, apart from the 3.6-60/40FR.

The highest values for both properties were found in the 3.0-100/0 and 3.0-80/20 mortars, which also have the highest values of $[H_2O] / [Na_2O]$ ratio (Table 3). In fact, water doesn't take part in the reaction, leaving voids inside the matrix after evaporation. These results are also in accordance with the results obtained during the mechanical characterization of the repair mortars presented in section 4.2.2.

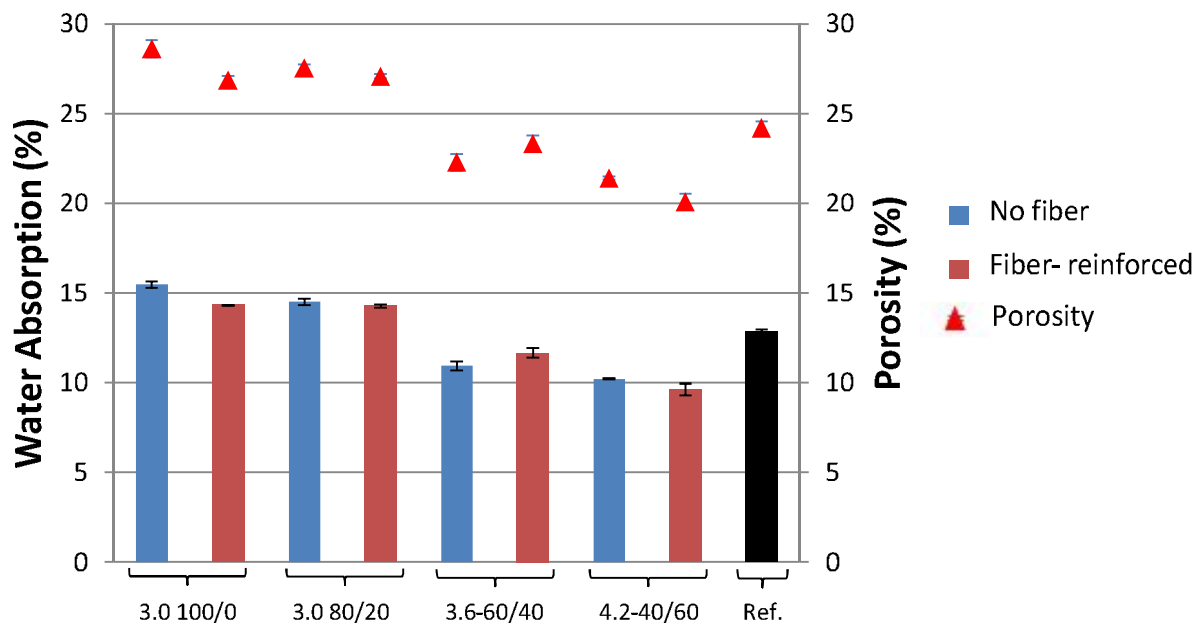


Figure 46 – Water absorption and apparent porosity

The apparent density of the alkali-activated repair mortar is presented in Figure 47, where the density is shown in function of the BFS content and compared to the solution / binder ratio. The values lie between 1.85 to 2.09 g/cm³ and the Ref. (commercial mortar) has a density of 1.89 g/cm³. The apparent density results are also in accordance with the porosity ones, i.e. denser mortars are also those with lower apparent porosity.

An important parameter for casting mortars based on Portland cement is the water / cement ratio (w/c). This parameter is analogue to the solution / binder (s/b) ratio for alkali-activated materials, playing an important role in the viscosity and in the consistency of the mixes (BORGES *et al.*, 2014). Figure 47 shows that the apparent density of the mortars is higher when the s/b is lower and the BFS content is higher; both help the matrix densification. The presence of fiber does not affect the water absorption, apparent porosity and density.

The results of the physical properties indicate that the poor performance of the repair mortar 4.2-40/60 (i.e. lower bond strength on pull-off and early crack development with consequent lower ultimate flexural strength) is not related to its physical properties, as this mortar presented higher density and lower porosity results. Bond between PC concrete substrate and alkali-activated mortar is likely to be proportional to the silicate content, although higher amounts of silicate are not feasible due to processing of the mix.

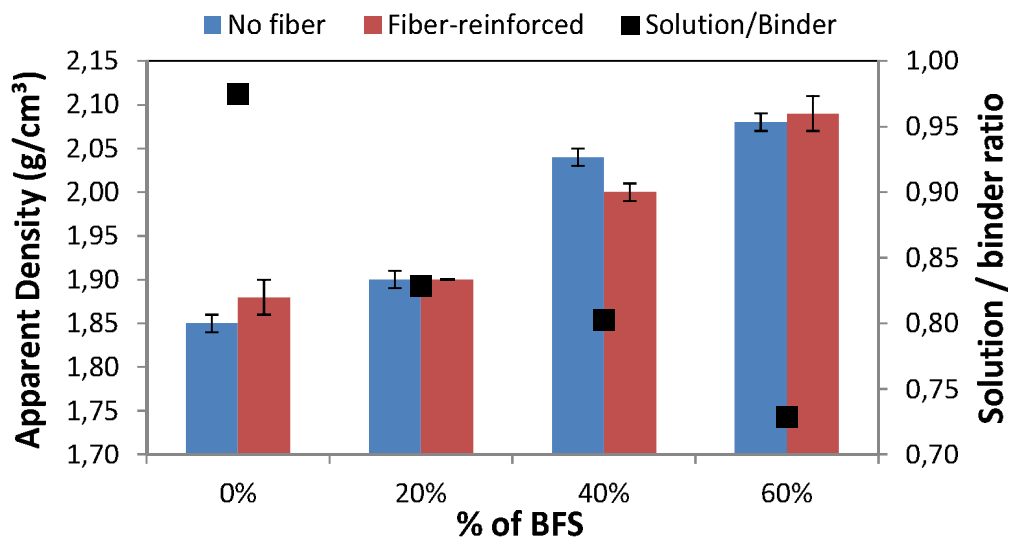


Figure 47 – Apparent density and solution/binder ratio versus % of BFS

5. CONCLUDING REMARKS

This research has focused on the development of an alternative repair mortars for concrete structures by assessing the compatibility and the adhesion between fiber-reinforced alkali-activated mortars and a concrete substrate.

In the first phase the focus was to pre-select some alkali-activated mortars based on their compatibility with the substrate, according to the structural requirements for repair materials. Twenty-one formulations had their properties evaluated (fresh and mechanical). For the fresh properties, the workability was assessed with the flow table test and all formulations had their consistency fixed to a chosen range considered standard, in order to ensure application of the mortars.

Regarding the mechanical properties, the compressive strength and the modulus of elasticity were evaluated. A wide range of compressive strength was obtained for different $[\text{SiO}_2] / [\text{Al}_2\text{O}_3]$ molar ratios and of BFS content. The majority of the formulations had their modulus of elasticity within 15-18 GPa, an intrinsic property of alkali-activated materials with N-A-S-(H) gel presence (NĚMEČEK *et al.*, 2011). According to the structural compatibility requirements, five formulations, (changing the $[\text{SiO}_2] / [\text{Al}_2\text{O}_3]$ ratio and the BFS content) were chosen for the adhesion evaluation; 3.0-100/0, 3.0-80/20, 3.6-60/40, 4.2-40/60 and 3.6-20/80.

In the second phase the focus was the adhesion evaluation between the repair mortars and the concrete substrate. The first step of this evaluation was the assessment of the adhesion bond by pull-off testing (the main and most common test for repair systems). This test gives important information concerning the repair material bond behavior, such as its maximum and average bond strength and the type of failure (EN, 1999).

The overall results showed a good adhesion between the alkali-activated repair mortars, as most of them (3.0-100/0, 3.0-100/0FR, 3.0-80/20, 3.0-80/20FR and 4.2-40/60FR) had strength above the required for classes R1, R2 and R3 for materials repair (EN, B., 2005). These alkali-activated mortars achieved better results than the commercial PC repair mortar. It is important to note that the fiber presence slightly increased the bond strength in most of the cases; but overall, PP fibers have a marked effect mainly when the bond strength is reduced and may be disregarded

when the mortar formulation is designed to have good bond strength with the substrate.

As the second part of the adhesion evaluation, the crack and delamination behaviors were assessed by the four-point bending test. This test has shown the high stiffness of the repair mortars (typical for brittle materials) and an increment of energy absorption capacity when the fiber was incorporated. The test has also indicated that the flexural strength is directly improved with the BFS addition, as long as there are significant amounts of silicate. Higher amounts of silicate and BFS will indeed increase the strength and stiffness of mortar; however, the rapid strength development is also associated with autogenous shrinkage problems, which is an issue for the development of durable repair mortars.

The concept of the trapping mechanism proposed by Lim and Li (1997) wasn't found in any of the tested mortar; one has to bear in mind that the test was originally developed for strain-hardening materials, which is not the case when PP fibers are used. Nevertheless, the employment of this test in this research was quite helpful to access delamination of the mortars.

Moreover, the mortars with 100% MK presented the delamination problem due to drying shrinkage prior the test. This is an issue already observed in the literature (ZANOTTI *et al.*, 2017). In fact, MK mortar should be avoided as repair materials for some important reasons. Firstly, repair mortars must be cured at room temperature (to allow in situ application), which is not helpful for the strength and stiffness development in MK-based AAM. As a consequence, the matrix cannot withstand any slight early deformation without cracking. This is even more critical because 100% MK-based AAM require higher solution to binder ratio (as a consequence of the fineness of MK). So, drying shrinkage takes place and delamination follows the shrinkage cracks, which develop before the mortars are tested.

Small additions of BFS will somehow help prevent this issue, as (i) the strength development and stiffness is increased at room temperature; (ii) the lower water demand reduced the susceptibility to drying shrinkage. In fact, BFS densifies the matrices, reducing the water porosity and increasing the density.

Combining the load-displacement behavior, the ultimate flexural strength and the cracking development pattern, we believe that an alkali-activated matrix containing 20% BFS as replacement for MK and with low $[\text{SiO}_2] / [\text{Al}_2\text{O}_3]$ (i.e. 3.0) presented the best performance for repair applications. This is the case of

formulation 3.0-80/20FR herein. Firstly, it has shown high bond strength in pull-off test; then it presented the best deformation capacity under stress (Figure 41), an acceptable ultimate flexural strength ($\sim 5.0\text{MPa}$ – 10% of its compressive strength) with a small variation between samples (Figure 43). Finally, it has shown an interesting crack development pattern in flexion, typical from good compatibility and adhesion between the repair mortar and the substrate (Figure 44).

REFERENCES

ABNT, N. 7215: Cimento Portland: determinação da resistência à compressão. **Rio de Janeiro**, 1996.

_____. 9778: Argamassa e concreto endurecidos—determinação da absorção de água, índice de vazios e massa específica. **Rio de Janeiro: Associação Brasileira de Normas Técnicas**, 2005.

_____. 5739: Concreto—Ensaio de compressão de Corpos-de-prova Cilíndricos. **Rio de Janeiro**, 2007.

_____. 8522: Concreto—Determinação do módulo estático de elasticidade à compressão. **Rio de Janeiro**, 2008.

_____. 7211: Agregado para concreto: Especificação. **Associação Brasileira de Normas Técnicas, Rio de Janeiro**, 2009.

_____. 13276: Argamassa para assentamento e revestimento de paredes e tetos—Preparo da mistura e determinação do índice de consistência. **Rio de Janeiro**, 2016.

ABNT, N. N. 248-Agregado—Determinação da composição Granulométrica. **Associação Brasileira de Normas Técnicas, Rio de Janeiro**, 2003.

AHMED, S. Fibre-reinforced geopolymer composites (FRGCs) for structural applications. In: (Ed.). **Advances in Ceramic Matrix Composites**: E-Publishing Inc. Cambridge, 2014. p.471-495.

ALANAZI, H. et al. Bond strength of PCC pavement repairs using metakaolin-based geopolymer mortar. **Cement and Concrete Composites**, v. 65, p. 75-82, 2016. ISSN 0958-9465.

BANTHIA, N. Report on the physical properties and durability of fiber-reinforced concrete. **ACI 544.5 R-10, Reported by ACI Committee 544**, p. 1-3, 2010. ISSN 0870313657.

BANTHIA, N.; GUPTA, R. Influence of polypropylene fiber geometry on plastic shrinkage cracking in concrete. **Cement and Concrete Research**, v. 36, n. 7, p. 1263-1267, 2006. ISSN 0008-8846.

BARICEVIC, A.; PEZER, M.; STIRMER, N. Utilization of polypropylene fibre reinforced cement composites as a repair material: A review. Concrete Repair, Rehabilitation and Retrofitting IV: Proceedings of the 4th International Conference on Concrete Repair, Rehabilitation and Retrofitting (ICCRRR-4), 5-7 October 2015, Leipzig, Germany, 2015, CRC Press. p.465.

BAYASI, Z.; ZENG, J. Properties of polypropylene fiber reinforced concrete. **Materials Journal**, v. 90, n. 6, p. 605-610, 1993. ISSN 0889-325X.

BERNAL, S. A. et al. Binder chemistry—high-calcium alkali-activated materials. In: (Ed.). **Alkali Activated Materials**: Springer, 2014. p.59-91. ISBN 9400776713.

BERNAL, S. A. et al. High-Resolution X-ray Diffraction and Fluorescence Microscopy Characterization of Alkali-Activated Slag-Metakaolin Binders. **Journal of the american ceramic society**, v. 96, n. 6, p. 1951-1957, 2013. ISSN 1551-2916.

BERNAL, S. A. et al. Mechanical and thermal characterisation of geopolymers based on silicate-activated metakaolin/slag blends. **Journal of materials science**, v. 46, n. 16, p. 5477, 2011. ISSN 0022-2461.

BERNAL, S. A. et al. Activation of metakaolin/slag blends using alkaline solutions based on chemically modified silica fume and rice husk ash. **Waste and Biomass Valorization**, v. 3, n. 1, p. 99-108, 2012. ISSN 1877-2641.

BIGNOZZI, M. C. et al. Mix-design and characterization of alkali activated materials based on metakaolin and ladle slag. **Applied Clay Science**, v. 73, p. 78-85, 2013. ISSN 0169-1317.

BORGES, P. H. et al. Performance of blended metakaolin/blastfurnace slag alkali-activated mortars. **Cement and Concrete Composites**, v. 71, p. 42-52, 2016. ISSN 0958-9465.

BORGES, P. H. et al. Andreasen particle packing method on the development of geopolymer concrete for civil engineering. **Journal of Materials in Civil Engineering**, v. 26, n. 4, p. 692-697, 2014. ISSN 0899-1561.

BUCHWALD, A.; HILBIG, H.; KAPS, C. Alkali-activated metakaolin-slag blends—performance and structure in dependence of their composition. **Journal of materials science**, v. 42, n. 9, p. 3024-3032, 2007. ISSN 0022-2461.

BUCHWALD, A.; TATARIN, R.; STEPHAN, D. Reaction progress of alkaline-activated metakaolin-ground granulated blast furnace slag blends. **Journal of materials science**, v. 44, n. 20, p. 5609-5617, 2009. ISSN 0022-2461.

DAVIDOVITS, J. Properties of geopolymer cements. First international conference on alkaline cements and concretes, 1994. p.131-149.

_____. **Method for bonding fiber reinforcement on concrete and steel structures and resultant products**: Google Patents 1999.

DAVIDOVITS, J.; DAVIDOVICS, M.; DAVIDOVITS, N. **Alkaline alumino-silicate geopolymeric matrix for composite materials with fiber reinforcement and method for obtaining same**: Google Patents 1998.

EMMONS, P. H.; VAYSBURD, A. M.; MCDONALD, J. E. Rational Approach to Durable Concrete Repairs. **Concrete International**, v. 15, n. 9, p. 40-45, 1993. ISSN 0162-4075.

EN. 1504 Products and systems for the protection and repair of concrete structures. 2005.

EN, B. 1504-3 Products and systems for the protection and repair of concrete structures. Definitions, requirements, quality control and evaluation of conformity. Structural and non-structural repair. **British Standard Institute**, 2005.

EN, B. S. 1542: 1999 Products and systems for the protection and repair of concrete structures. Test methods. Measurement of bond strength by pull-of. 1999.

FERNÁNDEZ-JIMÉNEZ, A.; PALOMO, J.; PUERTAS, F. Alkali-activated slag mortars: mechanical strength behaviour. **Cement and Concrete Research**, v. 29, n. 8, p. 1313-1321, 1999. ISSN 0008-8846.

GARCIA-LODEIRO, I.; PALOMO, A.; FERNÁNDEZ-JIMÉNEZ, A. 2 - An overview of the chemistry of alkali-activated cement-based binders. In: (Ed.). **Handbook of Alkali-Activated Cements, Mortars and Concretes**. Oxford: Woodhead Publishing, 2015. p.19-47. ISBN 978-1-78242-276-1.

GENCEL, O. et al. Mechanical properties of self-compacting concrete reinforced with polypropylene fibres. **Materials Research Innovations**, v. 15, n. 3, p. 216-225, 2011. ISSN 1432-8917.

GHODDOUSI, P.; JAVID, A. A. S. Plastic Shrinkage Evaluation of Self-Consolidating Concrete as Repair Materials Based on Restrained and Free Strain Measurements. In: (Ed.). **Design, Production and Placement of Self-Consolidating Concrete**: Springer, 2010. p.295-306.

HEAH, C. Y. et al. Kaolin-based geopolymers with various NaOH concentrations. **International Journal of Minerals, Metallurgy, and Materials**, v. 20, n. 3, p. 313-322, 2013. ISSN 1674-4799.

HU, S. et al. Bonding and abrasion resistance of geopolymeric repair material made with steel slag. **Cement and concrete composites**, v. 30, n. 3, p. 239-244, 2008. ISSN 0958-9465.

IDEKER, J.; BAÑUELOS, J. The use of synthetic blended fibers to reduce cracking risk in high performance concrete. **Final Report, Oregon Department of Transportation, Salem, Ore, USA**, 2014.

KHAN, M. I. et al. Effect of Na/Al and Si/Al Ratios on Adhesion Strength of Geopolymers as Coating Material. **Applied Mechanics & Materials**, n. 625, 2014. ISSN 1662-7482.

KRAMAR, S.; ŠAJNA, A.; DUCMAN, V. Assessment of alkali activated mortars based on different precursors with regard to their suitability for concrete repair. **Construction and Building Materials**, v. 124, p. 937-944, 2016. ISSN 0950-0618.

KUMAR, R.; GOEL, P.; MATHUR, R. Suitability of concrete reinforced with synthetic fiber for the construction of pavements. Proceedings of the 3rd International Conference on Sustainable Construction Materials and Technologies, 2013.

KURTZ, S.; BALAGURU, P.; DAVIDOVITS, J. Geopolymer composites layers for strengthening concrete structures. Proceedings of 2nd International Conference Geopolymer, 1999. p.173-180.

LAMOUR, V.; MORANVILLE, M.; CHAIGNON, J. Effect of low volume polypropylene fibers on early age cracking of concrete. ConMat'05-3d International Conference on Construction Materials: Performance, Innovations and Structural Implications, 2005.

LI, C.; SUN, H.; LI, L. A review: The comparison between alkali-activated slag (Si+Ca) and metakaolin (Si+ Al) cements. **Cement and Concrete Research**, v. 40, n. 9, p. 1341-1349, 2010. ISSN 0008-8846.

LI, V.; LIM, Y.; FOREMSKY, D. Interfacial fracture toughness of concrete repair materials. **Proceedings of Fracture Mechanics of Concrete Structures II, Aedificatio Publishers, Freiburg**, p. 1329-1344, 1995.

LIM, Y. M.; LI, V. C. Durable repair of aged infrastructures using trapping mechanism of engineered cementitious composites. **Cement and Concrete Composites**, v. 19, n. 4, p. 373-385, 1997. ISSN 0958-9465.

MAILVAGANAM, N. P. **Repair and protection of concrete structures**. 1992. ISBN 0849349931.

MAROSSZEKY, M. Stress performance in concrete repairs. International Conference on Rehabilitation of Concrete Structures, 1992, Melbourne, Victoria, Australia, 1992.

MASSON, G.; ALLEN, R. Cements and aggregates. **The Repair of Concrete Structures**, p. 34, 1993.

MENNA, C. et al. Use of geopolymers for composite external reinforcement of RC members. **Composites Part B: Engineering**, v. 45, n. 1, p. 1667-1676, 2013. ISSN 1359-8368.

MOMAYEZ, A. et al. Comparison of methods for evaluating bond strength between concrete substrate and repair materials. **Cement and concrete research**, v. 35, n. 4, p. 748-757, 2005. ISSN 0008-8846.

MORGAN, D. Compatibility of concrete repair materials and systems. **Construction and building materials**, v. 10, n. 1, p. 57-67, 1996. ISSN 0950-0618.

MYERS, D.; KANG, T. H.; RAMSEYER, C. Early-age properties of polymer fiber-reinforced concrete. **International Journal of Concrete Structures and Materials**, v. 2, n. 1, p. 9-14, 2008. ISSN 1976-0485.

NAAMAN, A. E.; WONGTANAKITCHAROEN, T.; HAUSER, G. Influence of different fibers on plastic shrinkage cracking of concrete. **ACI materials Journal**, v. 102, n. 1, p. 49-58, 2005. ISSN 0889-325X.

NĚMEČEK, J.; ŠMILAUER, V.; KOPECKÝ, L. Nanoindentation characteristics of alkali-activated aluminosilicate materials. **Cement and Concrete Composites**, v. 33, n. 2, p. 163-170, 2011. ISSN 0958-9465.

PACHECO-TORGAL, F. et al. An overview on the potential of geopolymers for concrete infrastructure rehabilitation. **Construction and Building Materials**, v. 36, p. 1053-1058, 2012. ISSN 0950-0618.

PACHECO-TORGAL, F.; CASTRO-GOMES, J.; JALALI, S. Adhesion characterization of tungsten mine waste geopolymeric binder. Influence of OPC concrete substrate surface treatment. **Construction and Building Materials**, v. 22, n. 3, p. 154-161, 2008a. ISSN 0950-0618.

PACHECO-TORGAL, F.; CASTRO-GOMES, J.; JALALI, S. Alkali-activated binders: A review: Part 1. Historical background, terminology, reaction mechanisms and hydration products. **Construction and Building Materials**, v. 22, n. 7, p. 1305-1314, 2008b. ISSN 0950-0618.

PACHECO-TORGAL, F. et al. **Handbook of alkali-activated cements, mortars and concretes**. Elsevier, 2015. ISBN 1782422889.

PATEL, P. A.; DESAI, A. K.; DESAI, J. A. Evaluation of engineering properties for polypropylene fiber reinforced concrete. **International journal of advanced engineering technology**, v. 3, n. 1, p. 42-45, 2012.

PROVIS, J. L. Alkali-activated materials. **Cement and Concrete Research**, 2017. ISSN 0008-8846.

PROVIS, J. L.; BERNAL, S. A. Binder chemistry-blended systems and intermediate Ca content. In: (Ed.). **Alkali Activated Materials**: Springer, 2014a. p.125-144.

_____. Geopolymers and related alkali-activated materials. **Annual Review of Materials Research**, v. 44, p. 299-327, 2014b. ISSN 1531-7331.

PROVIS, J. L. et al. **Durability and Testing–Physical Processes**. Alkali Activated Materials: Springer: 277-307 p. 2014.

PROVIS, J. L. et al. Binder Chemistry–Low-Calcium Alkali-Activated Materials. In: (Ed.). **Alkali Activated Materials**: Springer, 2014. p.93-123.

PROVIS, J. L.; VAN DEVENTER, J. S. J. Alkali Activated Materials: State-of-the-Art **RILEM TC 224-AAM**, v. 13, 2014.

PUERTAS, F.; FERNÁNDEZ-JIMÉNEZ, A. Mineralogical and microstructural characterisation of alkali-activated fly ash/slag pastes. **Cement and Concrete composites**, v. 25, n. 3, p. 287-292, 2003. ISSN 0958-9465.

RAUPACH, M.; BUTTNER, T. **Concrete Repair to EN 1504 - Diagnosis, Design, Principles and Practice**. CRC Press, 2014. ISBN 9781466557468.

SAJE, D. et al. Autogenous and drying shrinkage of fibre reinforced high-performance concrete. **Journal of Advanced Concrete Technology**, v. 10, n. 2, p. 59-73, 2012. ISSN 1347-3913.

SAMSON, G.; CYR, M.; GAO, X. X. Formulation and characterization of blended alkali-activated materials based on flash-calcined metakaolin, fly ash and GGBS. **Construction and Building Materials**, v. 144, p. 50-64, 2017. ISSN 0950-0618.

SEFEROVIĆ, E. Polypropylene fibers in the support work for the Sveti Rok tunnel. **Građevinar**, v. 54, n. 09., p. 535-539, 2002. ISSN 0350-2465.

SHAW, J. Polymers for concrete repair. **The Repair of Concrete Structures**, p. 37-55, 1993. ISSN 0751400866.

SKAZLIĆ, M. **Hybrid high performance fibre-reinforced concrete**. 2003. Građevinski fakultet, Sveučilište u Zagrebu

SONG, P.; HWANG, S.; SHEU, B. Strength properties of nylon-and polypropylene-fiber-reinforced concretes. **cement and concrete research**, v. 35, n. 8, p. 1546-1550, 2005. ISSN 0008-8846.

VASCONCELOS, E. et al. Concrete retrofitting using metakaolin geopolymer mortars and CFRP. **Construction and Building Materials**, v. 25, n. 8, p. 3213-3221, 2011. ISSN 0950-0618.

WALLAH, S. E.; HARDJITO, D. Assessing the shrinkage and creep of alkali-activated concrete binders. **Handbook of alkali-activated cements, mortars and concretes**, p. 265-287, 2015.

WANG, W.-C.; WANG, H.-Y.; LO, M.-H. The fresh and engineering properties of alkali activated slag as a function of fly ash replacement and alkali concentration. **Construction and Building Materials**, v. 84, p. 224-229, 2015. ISSN 0950-0618.

ZANOTTI, C. et al. Bond strength between concrete substrate and metakaolin geopolymer repair mortar: Effect of curing regime and PVA fiber reinforcement. **Cement and Concrete Composites**, 2017. ISSN 0958-9465.

ZHANG, H. Y. et al. Characterizing the bond strength of geopolymers at ambient and elevated temperatures. **Cement and Concrete Composites**, v. 58, p. 40-49, 2015. ISSN 0958-9465.

ZHANG, Z.; WANG, H. Alkali-activated cements for protective coating of OPC concrete. 2015. ISSN 1782422765.



PPGEC – Programa de Pós Graduação em Engenharia Civil
Av Amazonas, 7675, Belo Horizonte-MG
www.civil.cefetmg.br/mestrado